universe

IMPACT FACTOR 2.5

CITESCORE 4.3

Article

Starobinsky Inflation with T-Model Kähler Geometries

Constantinos Pallis

Special Issue

Particle Physics and Cosmology: A Themed Issue in Honor of Professor Dimitri Nanopoulos

Edited by

Prof. Dr. Jun-Jie Cao, Prof. Dr. Yungui Gong, Prof. Dr. Tianjun Li and Dr. Natsumi Nagata

MDPI

https://doi.org/10.3390/universe11030075

universe

MDPI

Article

Starobinsky Inflation with T-Model Kähler Geometries

Constantinos Pallis

School of Technology, Aristotle University of Thessaloniki, GR-541 24 Thessaloniki, Greece; kpallis@auth.gr

Abstract: We present novel implementations of Starobisky-like inflation within supergravity adopting Kähler potentials for the inflaton which parameterizes hyperbolic geometries known from T-model inflation. The associated superpotentials are consistent with an R and a global or gauge $U(1)_X$ symmetries. The inflaton is represented by a gauge-singlet or non-singlet superfield and is accompanied by a gauge-singlet superfield successfully stabilized thanks to its compact contribution into the total Kähler potential. Keeping the Kähler manifold intact, a conveniently violated shift symmetry is introduced which allows for slight variation in the predictions of Starobinsky inflation: The (scalar) spectral index exhibits an upper bound which lies close to its central observational value whereas the constant scalar curvature of the inflaton-sector Kähler manifold increases with the tensor-to-scalar ratio.

Keywords: cosmology; inflation; supersymmetric models

PACS: 98.80.Cq; 12.60.Jv; 95.30.Cq; 95.30.Sf

1. Introduction

Starobinsky inflation (SI) [1] stands out among the remaining viable inflationary models (for reviews, see refs. [2–5]) thanks to its simplicity, elegance, and observational success. Despite its original realization by the (arbitrary) addition of the $\mathcal{R}^2$ term—where $\mathcal{R}$ is the Ricci scalar—to the standard Einstein action, this inflationary model can be also driven by a scalar field with a suitable potential. Indeed, it is well known that gravity theories based on higher derivative terms of the type $\mathcal{R}^m$ with $m > 1$ are equivalent to standard gravity theories with one additional scalar degree of freedom [6]. From the proposed particle physics incarnations of this inflationary model (and its variant called α-SI) (for reviews, see refs. [7–10]) prominent position occupies its embedding within *Supergravity* (SUGRA) which is the natural extension of *Supersymmetry* (SUSY) to planckian mass scales [11]. Despite the fact that SUSY is not yet discovered at LHC [12], its presence—probably at higher energies—is a natural and mostly inevitable consequence of superstring theory [13]. Even without direct experimental signatures, SUSY has constructive impact on the stabilization of the electroweak vacuum and on several problems of modern particle cosmology such as inflation, baryogenesis and dark matter.

Trying to classify the most popular SUGRA realizations of SI, we can single out indicatively the following categories (for alternatives see, e.g., refs. [6,14–18]):

- Wess–Zumino models with a matter-like inflaton [19–24]. Polynomial superpotentials, W—of the Wess–Zumino form [11]—are adopted in this class of models and the Kähler potentials K parameterize specific Kähler manifolds of the form $SU(N_{\rm m},1)/SU(N_{\rm m})\times U(1)$, inspired by the no-scale models [25,26] of SUSY breaking. The stabilization of the inflaton-accompanying modulus at a Planck-scale value [20] is achieved by a deformation of the internal geometry.

Academic Editors: Jun-Jie Cao, Yungui Gong, Tianjun Li and Natsumi Nagata

Received: 1 February 2025
Revised: 15 February 2025
Accepted: 18 February 2025
Published: 21 February 2025

Citation: Pallis, C. Starobinsky Inflation with T-Model Kähler Geometries. *Universe* **2025**, *11*, 75. https://doi.org/10.3390/universe11030075

- Ceccoti-like [27] models with a modulus-like inflaton [20,28–37]. Similar K's are used here whereas W is linear [38] with respect to the matter-like inflaton-accompanying field which may be stabilized at the origin via several mechanisms [6,10,35,39–43]. In a subclass of these models [31–34,36,37], the conjecture of induced gravity [44,45] is incorporated leading to a dynamical generation of the reduced Planck scale, $m_{\rm P}$ through the *vacuum expectation value* (v.e.v) of the inflaton at the end of its evolution.
- Models with a strong linear non-minimal coupling to gravity [46–48]—or a strong linear contribution into this coupling [49]—remain unitarily safe [50] up to the Planck scale.
- Models which exhibit a pole [51–55] of order *one* in the kinetic term of the inflaton [56–58]. As in every SI model, the inflationary potential develops one shoulder for large $\widehat{\phi}$ values, where $\widehat{\phi}$ is the canonically normalized inflaton which can be expressed in terms of the original field ϕ as [58]

$$\phi = 1 - e^{-\sqrt{2/N}\widehat{\phi}} \quad (\text{: E-Model Normalization}). \tag{1}$$

  The presence of the real positive variable N—aligned to the conventions of ref. [58]—leads to a generalized version of SI called α-SI [20] or *E-Model* inflation. This model can be contrasted with the *T-Model* inflation [59,60] which arises thanks to a pole of order *two* in the inflaton kinetic term and features a potential with two symmetric plateaus away from the origin. Namely, the $\phi - \widehat{\phi}$ relation assumes the form

$$\phi = \tanh\left(\widehat{\phi}/\sqrt{2N}\right) \quad (\text{: T-Model Normalization}). \tag{2}$$

  Independently of their particularities, both models share [8] common predictions for the inflationary observables and for this reason they are called collectively α-attractors [5,61–63].

In our present investigation, stimulated by ref. [60] (see also ref. [64]) we propose another embedding of SI within $\mathcal{N} = 1$ standard Poincaré SUGRA that is exclusively based on the presence of a pole of order *two* in the inflaton kinetic term, i.e., it is based on the $\phi - \widehat{\phi}$ relation of Equation (2). Namely, the scalar potential, expressed in terms of the initial (non-canonical) inflaton, ϕ, is written as

$$V_{\rm I} = \lambda^2(\phi^{n/2} - M^2)^2/(1+\phi)^{n_{\rm d}} \quad \text{with} \quad M \ll m_{\rm P} = 1. \tag{3}$$

For $n = n_{\rm d} = 2$, $V_{\rm I}$ has been motivated in Refs. [29,60] via a breaking of conformal symmetry in a non-SUSY framework. It also appears in unified models of no-scale α-SI with SUSY breaking [65]. Here, we extend the analysis in the context of SUGRA, providing a method which allows the generation of $V_{\rm I}$ from conveniently selected W and K. Our particle content includes, in addition to the inflaton superfield(s), an extra gauge-singlet superfield which assist in the stabilization of the SUGRA potential during SI [38]. Moreover, we employ monomial W's consistent with an R and a global or gauge $U(1)_X$ symmetry. On the other hand, the K's respect the R and the gauge symmetry and are *holomorphically* equivalent to those yielding Equation (2) [56,66–68]. In other words, K has the well-known form employed in T-model inflation [56,66] up to a number of extra holomorphic and anti-holomorphic terms which do not influence the resulting Kähler metric. The one pair of these terms endows K with a shift symmetry which facilitates the performance of inflation [56,66–68]. The second pair provides a breaking of the aforementioned shift symmetry which is already violated mildly in W. Both violations are natural in the 't Hooft sense [69] for sufficiently low values of the exponent $n_{\rm d}$ in K and the coupling constant λ entered in W. The particular importance of an enhanced shift symmetry in taming the

so-called η-problem of inflation in SUGRA is already recognized for gauge singlets, e.g., in refs. [70–75] and non-singlets, e.g., in refs. [36,48,76–79].

Compared to the aforementioned implementations of SI within SUGRA, the present version assures a totally symmetric Kähler manifold together with a simple W. Let us recall that polynomial W's with R symmetry are reconciled with a K which does not parameterize specific Kähler manifold in Ref. [58] whereas totally symmetric K's usually require complicate W's (see, e.g., refs. [20,30,56,57,61]). On the contrary, the W's employed here are very common in particle physics and so the inflaton can be easily identified with a field already present in the theory, e.g., the right-handed sneutrino [70,80–82] or a superheavy Higgs superfield responsible for the spontaneous breaking of a gauge symmetry [36,37]. Also, it is expected that this scheme assures naturally a low enough reheating temperature, potentially consistent with the gravitino constraint and non-thermal leptogenesis [31,36,37,83,84] if connected with a version of the *Minimal SUSY Standard Model* (MSSM). Furthermore, our proposal does not require tuning of parameters other than a mild one to the initial conditions, it is not based on any conjecture such as that of induced gravity [10,31–37], and it provides a relative flexibility regarding the observables. Lastly, it offers us the opportunity to exemplify Kähler potential engineering, which allows us to obtain the various desired factors of $V_{\rm I}$ in Equation (3) together with a desirable Kähler metric.

We describe below how we can formulate SI in the context of SUGRA in Section 2 and we specify two versions of SI: one employing a gauge-singlet inflaton in Section 3 called for short *Chaotic Starobinsky inflation* (CSI) and one with a gauge-non-singlet inflaton called *Higgs Starobinsky inflation* (HSI) since it causes the breaking of a gauge symmetry (see Section 4). Our conclusions are summarized in Section 6. In Appendix A, we demonstrate that our proposed K's enjoy an enhanced shift symmetry. Throughout the text, the subscript χ denotes derivation *with respect to* the field χ and charge conjugation is denoted by a star (*). Unless otherwise stated, we use units where the reduced Planck scale $m_{\rm P} = 2.4 \cdot 10^{18}$ GeV is set equal to unity.

2. SUGRA Framework

We start our investigation presenting the basic formulation of a scalar theory within SUGRA in Section 2.1 and then, in Section 2.2, we outline our strategy in constructing our models of SI.

2.1. General Setup

The part of the (Einstein-frame) action within SUGRA which describes the (complex) scalar fields z^α coupled minimally to Einstein gravity can be written as [11]

$$\mathcal{A} = \int d^4x\sqrt{-\mathfrak{g}}\left(-\frac{1}{2}\mathcal{R} + K_{\alpha\bar{\beta}}D_\mu z^\alpha D^\mu z^{*\bar{\beta}} - V_{\rm SUGRA}\right), \tag{4a}$$

where $\mathcal{R}$ is the space-time Ricci scalar curvature, $\mathfrak{g}$ is the determinant of the Friedmann–Robertson–Walker metric, $g_{\mu\nu}$, with signature $(+,-,-,-)$. Also, summation is taken over the scalar fields z^α which are denoted by the same symbol of the corresponding superfield. The kinetic mixing of z^α is controlled by the Kähler potential K and the relevant metric defined as

$$K_{\alpha\bar{\beta}} = K_{,z^\alpha z^{*\bar{\beta}}} > 0 \ \text{ with } \ K^{\bar{\beta}\alpha}K_{\alpha\bar{\gamma}} = \delta^{\bar{\beta}}_{\bar{\gamma}}. \tag{4b}$$

Also, the covariant derivatives for the z^α's are given by

$$D_\mu z^\alpha = \partial_\mu z^\alpha + igA^{\rm a}_\mu T^{\rm a}_{\alpha\beta} z^\beta \tag{4c}$$

with A^{a}_{μ} being the vector gauge fields, g the (unified) gauge coupling constant and T^{a} with $\mathrm{a} = 1, \ldots, \mathrm{dim}G_{\mathrm{GUT}}$ the generators of a gauge group G_{GUT}.

Finally $\mathcal{A}$ contains the SUGRA scalar potential, V_{SUGRA}, which is given in terms of K, and the superpotential, W, by

$$V_{\mathrm{SUGRA}} = V_{\mathrm{F}} + V_{\mathrm{D}} \ \text{ with } \ V_{\mathrm{F}} = e^{K}\left(K^{\alpha\bar{\beta}}\mathrm{F}_{\alpha}\mathrm{F}^{*}_{\bar{\beta}} - 3|W|^{2}\right) \ \text{ and } \ V_{\mathrm{D}} = g^{2}\sum_{\mathrm{a}}\mathrm{D}_{\mathrm{a}}\mathrm{D}_{\mathrm{a}}/2, \quad (4\mathrm{d})$$

where a trivial gauge kinetic function is adopted whereas the F- and D-terms read

$$\mathrm{F}_{\alpha} = W_{,z^{\alpha}} + K_{,z^{\alpha}}W \ \text{ and } \ \mathrm{D}_{\mathrm{a}} = z_{\alpha}(T_{\mathrm{a}})^{\alpha}_{\beta}K^{\beta} \ \text{ with } \ K^{\alpha} = K_{,z^{\alpha}}\,. \quad (4\mathrm{e})$$

As we emphasized in Section 1, SI in our work is attained by deriving V_{I} in Equation (3) from V_{SUGRA} and not modifying gravity which remains at the minimal level as shown from the absence of higher order $\mathcal{R}$ terms in Equation (4a). Therefore, our next task is to select conveniently the functions K and W so that Equations (2) and (3) are reproduced.

2.2. Guidelines

We embark on describing our procedure to obtain the desired V_{I} in Equation (3) from V_{F} in Equation (4d) and the desired $\phi - \widehat{\phi}$ relation in Equation (2). Although our presentation in adapted to our present model, the strategy of our approach has a wider applicability suitable for other cases.

2.2.1. Achieving D-Flatness

Our final aim is the derivation of V_{I} in Equation (3) through V_{F} in Equation (4d). This decision requires the establishment of D-flatness during SI, i.e., $\langle V_{\mathrm{D}}\rangle_{\mathrm{I}} = 0$—where $\langle Q\rangle_{\mathrm{I}}$ symbolizes the value of the quantity Q during inflation. Assuming that the gauge non-singlet superfields are placed at zero during inflation, D-flatness may be attained in the following two cases:

- If the inflaton is (the radial part of) a gauge-singlet superfield $z^2 := \Phi$. In this case, Φ has obviously zero contribution to V_{D}.
- If the inflaton is the radial part of a conjugate pair of Higgs superfields, $z^2 := \Phi$ and $z^3 := \bar{\Phi}$, in the fundamental representation of G_{GUT}. In such a case (see Section 4.3 below) we obtain $\langle V_{\mathrm{D}}\rangle_{\mathrm{I}} = 0$. The same result can be obtained if G_{GUT} is more structured than $U(1)_X$ employing just one superfield z^2 in the adjoint representation of G_{GUT} and using as inflaton its neutral component(see e.g., ref. [85]).

2.2.2. Selecting the Suitable W

Despite the fact that V_{I} in Equation (3) includes only one field, its derivation from V_{F} is facilitated [38] if W includes at least two fields from which the first $z^1 := S$ is a gauge-singlet superfield called a stabilizer or goldstino. The latter is due to the fact that for $S = 0$ SUSY is broken since $\langle F_S\rangle_{\mathrm{I}} \neq 0$. The presence of S serves the following purposes:

- It assists in determining W. To achieve it, we require that S appears linearly in W and so both are equally charged under a global R symmetry.
- It can be stabilized at $\langle S\rangle_{\mathrm{I}} = 0$ without invoking higher order terms, if we select [35]

$$K_2 = N_S \ln\left(1 + |S|^2/N_S\right) \ \Rightarrow \ \langle K_2^{SS^*}\rangle_{\mathrm{I}} = 1 \ \text{ with } \ 0 < N_2 < 6. \quad (5)$$

The index 2 stems from the fact that K_{s} parameterizes the compact manifold $SU(2)/U(1)$ [35]. Note that for $\langle S\rangle_{\mathrm{I}} = 0$, S is canonically normalized and so we

do not care about its kinetic normalization henceforth. For other stabilization methods of S see refs. [6,39–43].

- It assures the boundedness of $V_{\rm I}$. Indeed, if we set $\langle S\rangle_{\rm I}=0$, then $\langle W_{,z^\alpha}\rangle_{\rm I}=0$ for $\alpha\neq 1$, $\langle K_{,z^\alpha}W\rangle_{\rm I}=0$ and $-3|\langle W\rangle_{\rm I}|^2=0$. Obviously, non-vanishing values of the last term may render $V_{\rm F}$ unbounded from below.
- It generates for $\langle S\rangle_{\rm I}=0$ and for monomial W the numerator of $V_{\rm I}$ in Equation (3) via the only term of $V_{\rm F}$ which remains "alive". Indeed, we obtain

$$V_{\rm I}:=\langle V_{\rm F}\rangle_{\rm I}=\langle e^K K^{SS^*}|W_{,S}|^2\rangle_{\rm I}. \tag{6}$$

Assuming that no mixing terms between S and the inflaton exist in K, we obtain $\langle K^{SS^*}\rangle_{\rm I}=\langle K_2^{SS^*}\rangle_{\rm I}=1$, and so the numerator of $V_{\rm I}$ in Equation (3) emerges if W has the form

$$W=SF_{\rm W}(z^\alpha)\quad\text{with}\quad\langle F_{\rm W}\rangle_{\rm I}=:f_{\rm W}=\lambda\phi^{n/2}\quad\text{and}\quad\phi=\mathsf{Re}\Phi, \tag{7}$$

given that the assumption $\langle\mathsf{Im}\Phi\rangle_{\rm I}=0$ yields mostly stable configuration; here, we focus on a gauge-singlet Φ. On the other hand, the denominator of $V_{\rm I}$ in Equation (3) may be generated via the exponential prefactor in Equation (6) through logarithmic contributions to K, as we explain below.

2.2.3. Selecting the Convenient Kähler Potential

The form of K has to accomplish the following two goals:

- It has to generate the desired $\phi-\widehat{\phi}$ relation in Equation (2). Therefore, we need to introduce a contribution into K including z^α and $z^{*\alpha}$ in the same function. After inspection (see Appendix of ref. [86]) we infer that a pole of order two in the kinetic term of inflaton is achieved if $K=K_{\rm T}$ where

$$K_{\rm T}=-N\ln F_{\rm T}(z^\alpha,z^{*\bar\beta})\quad\text{with}\quad\langle K_{\alpha\bar\beta}\rangle_{\rm I}=N/f_{\rm T}^2\quad\text{and}\quad f_{\rm T}:=\langle F_{\rm T}\rangle_{\rm I}=1-\phi^2. \tag{8}$$

Here, $N>0$ and the subscript "T" indicates that this part of the total K is responsible for the T-model Kähler metric (see Equation (4b)). However, from Equation (6), we remark that K affects—in addition to the kinetic mixing—$V_{\rm I}$ via the prefactor $e^{K_{\rm T}}$. Therefore, $F_{\rm T}$ is generically expected to emerge also in the denominator of $V_{\rm I}$ making difficult the establishment of an inflationary era. This problem can be surpassed [58,66] by two alternative strategies:

  - Adjusting W and constraining the prefactor of K in Equation (8), so that the pole is removed from $V_{\rm F}$ thanks to cancellations [19,54,58,66]. This recipe introduces some tuning, though, in the coefficients of W and, for this reason, we do not pursue this method here.
  - Replacing $K_{\rm T}$ with $\widetilde{K}_{\rm T}$ so that the desired kinetic terms in Equation (4a) remain unaltered and, simultaneously [56,58,66]

$$\langle e^{\widetilde{K}_{\rm T}}\rangle_{\rm I}=1\;\Leftrightarrow\;\langle\widetilde{K}_{\rm T}\rangle_{\rm I}=0\quad\text{with}\quad\widetilde{K}_{\rm T}=K_{\rm T}+K_{\rm sh}. \tag{9a}$$

In other words, the symmetry of $K_{\rm T}$ is augmented by some shift symmetry (see Appendix A) without disturbing $K_{\alpha\bar\beta}$ in Equation (4b). To accomplish this, $K_{\rm sh}$ includes holomorphic and anti-holomorphic terms which yield vanishing

contribution to the mixed derivatives of $\widetilde{K}_{\rm T}$. Taking into account the form of $K_{\rm T}$ in Equation (8), we may select formally

$$K_{\rm sh} = (N/2)\ln F_{\rm sh} + (N/2)\ln F_{\rm sh}^{*} \quad \text{with} \quad \langle F_{\rm sh}\rangle_{\rm I} =: f_{\rm sh} = f_{\rm T}. \tag{9b}$$

Note that the same construction is valid even in case of polynomial K's if we check the structure of the relevant K's in refs. [70,74–79].

- It has to generate the denominator of $V_{\rm I}$ in Equation (3). To achieve this, we focus on the exponential prefactor of $V_{\rm I}$ in Equation (6) and we demand

$$\langle e^{K_{\rm d}}\rangle_{\rm I} = (1+\phi)^{-n_{\rm d}}, \tag{10a}$$

where $K_{\rm d}$ has the following structure (similar to that of $K_{\rm sh}$)

$$K_{\rm d} = -(n_{\rm d}/2)\ln F_{\rm d} - (n_{\rm d}/2)\ln F_{\rm d}^{*} \quad \text{with} \quad \langle F_{\rm d}\rangle_{\rm I} =: f_{\rm d} = 1+\phi. \tag{10b}$$

so that it does not disrupt $K_{\alpha\bar{\beta}}$ in Equation (4b).

To recapitulate this section, we summarize that the adopted W in this work has the form in Equation (7) whereas the total K can be written as

$$\widetilde{K}_{\rm 2Td} = K_2 + \widetilde{K}_{\rm T} + K_{\rm d} \quad \text{with} \quad \widetilde{K}_{\rm T} = K_{\rm T} + K_{\rm sh}. \tag{11}$$

Below, we specify the functional forms of the related functions $F_{\rm T}$, $F_{\rm sh}$, and $F_{\rm d}$ for the two classes of SI considered, CSI, and HSI.

3. Gauge-Singlet Inflaton

We focus first on the case of CSI and we present in Section 3.1 the building blocks of the model. Then, we verify that the adopted K and W produce the desired kinetic mixing in Section 3.2 and inflationary potential in Section 3.3.

3.1. Setup

According to the strategy described in Section 2.2, the present setting is realized in presence of two gauge-singlet superfields S and Φ which may be parameterized as

$$\Phi = \phi\, e^{i\theta} \quad \text{and} \quad S = (s + i\bar{s})/\sqrt{2}. \tag{12}$$

The inflationary trajectory can be defined by the constraints

$$\langle S\rangle_{\rm I} = \langle \Phi - \Phi^{*}\rangle_{\rm I} = 0, \ \text{ or } \ \langle s\rangle_{\rm I} = \langle \bar{s}\rangle_{\rm I} = \langle \theta\rangle_{\rm I} = 0. \tag{13}$$

Following our plan in Section 2.2.2, we adopt a monomial W consistent with Equation (7) with the following structure

$$F_{\rm W} = \lambda\Phi^{n/2} \quad \text{and so} \quad W = \lambda S\Phi^{n/2}, \tag{14}$$

where λ is a free parameter, and n takes even values that preserve the holomorphicity of W. The form of W can be uniquely determined if we impose an R symmetry, under which S and Φ have charges 1 and 0 and a global $U(1)_X$ symmetry with assigned charges $Q_X(S) = -1$ and $Q_X(\Phi) = 2/n$. However, the latter is violated in the proposed K which

assumes the form in Equation (11) with the functions defined in Equations (8), (9b) and (10b) identified as follows:

$$F_{\rm T} = 1 - |\Phi|^2,\ F_{\rm sh} = 1 - \Phi^2 \ \text{ and } \ F_{\rm d} = 1 + \Phi. \tag{15}$$

Consequently, the total K takes the form

$$\widetilde{K}_{211{\rm d}} = K_2 + \widetilde{K}_{11} + K_{\rm d}, \tag{16}$$

where the individual contributions are specified as

$$\widetilde{K}_{11} = -N \ln \frac{1 - |\Phi|^2}{\sqrt{(1-\Phi^2)(1-\Phi^{*2})}} \ \text{ and } \ K_{\rm d} = -\frac{n_{\rm d}}{2}\ln(1+\Phi) - \frac{n_{\rm d}}{2}\ln(1+\Phi^*). \tag{17}$$

$\widetilde{K}_{211{\rm d}}$ parameterizes [56] the Kähler manifold $\mathcal{M}_{211}$ with moduli-space scalar curvature R_{211} given by

$$\mathcal{M}_{211} = (SU(2)/U(1))_S \times (SU(1,1)/U(1))_\Phi \ \text{ and } \ \mathsf{R}_{211} = -2/N + 2/N_S. \tag{18}$$

The indices in the product of Equation (18) indicate the moduli which parameterize the corresponding manifolds. Needless to say, $K_{\rm d}$ and the denominator in $\widetilde{K}_{11}$ have no impact on $\mathcal{M}_{211}$, as explained in Section 2.2.3, and violate the global $U(1)_X$ symmetry that is valid at the level of W.

3.2. Canonical Normalization

The first step towards the establishment of CSI is the canonical normalization of the fields involved in the parametrization of Φ in Equation (12). This can be performed if we identify the kinetic term on Equation (4a) with the canonical ones as follows:

$$\langle K_{\Phi\Phi^*}\rangle_{\rm I}|\dot{\Phi}|^2 \simeq \frac{1}{2}\left(\dot{\widehat{\phi}}^2 + \dot{\widehat{\theta}}^2\right) \ \Rightarrow \ \frac{d\widehat{\phi}}{d\phi} = J = \frac{\sqrt{2N}}{f_{\rm T}} \ \text{ and } \ \widehat{\theta} \simeq J\phi\theta \ \text{ with } \ \langle K_{\Phi\Phi^*}\rangle_{\rm I} = \frac{N}{f_{\rm T}^2}, \tag{19}$$

found from Equation (A3) if we restrict our attention on the path in Equation (13). Upon integrating the $\phi - \widehat{\phi}$ relation above, we arrive at Equation (2) in accordance with our aim.

3.3. Inflationary Potential

The second step in our attempt to implement SI is the reproduction of $V_{\rm I}$ of Equation (3) starting from Equation (6) with W given in Equation (14) and $K = \widetilde{K}_{211{\rm d}}$ in Equation (16). This is trivially verified if we take into account the field configuration of Equation (13). However, $V_{\rm I}$ of Equation (3) is a tree-level result which may receive radiative corrections. These can be estimated by constructing the mass spectrum of the theory along the trajectory in Equation (13). Our results are summarized in Table 1, where we arrange the expressions of the masses squared $\widehat{m}^2_{\chi^\alpha}$ (with $\chi^\alpha = \theta$ and s) divided by $H_{\rm I}^2 \simeq V_{\rm I}/3$. From them, we can appreciate the role of $N_S < 6$ in retaining positive $\widehat{m}^2_s$ and thereby stabilizing the track in Equation (13). Also, we confirm that $\widehat{m}^2_{\chi^\alpha} \gg H_{\rm I}^2$ for $\phi \leq 1$, and so we do not obtain inflationary primordial perturbation from other fields in addition to ϕ. In Table 1, we display also the masses $\widehat{m}^2_{\psi_\pm}$ of the corresponding fermions. We define $\widehat{\psi}_\Phi = J\psi_\Phi$ where ψ_Φ and ψ_S are the Weyl spinors associated with S and Φ, respectively. Considering SUGRA as an effective theory with cutoff scale equal to $m_{\rm P}$, the well-known Coleman–Weinberg formula (see, e.g., ref. [77]) can be employed self-consistently taking into account the masses

which lie well below $m_{\rm P}$, i.e., all the masses arranged in Table 1. Therefore, the one-loop correction to $V_{\rm I}$ reads

$$\Delta V_{\rm I} = \frac{1}{64\pi^2}\left(\widehat{m}_\theta^4 \ln\frac{\widehat{m}_\theta^2}{\Lambda^2} + 2m_s^4 \ln\frac{m_s^2}{\Lambda^2} - 4\widehat{m}_{\psi_\pm}^4 \ln\frac{\widehat{m}_{\psi_\pm}^2}{\Lambda^2}\right), \tag{20}$$

where Λ is a *renormalization group* (RG) mass scale. The resulting $\Delta V_{\rm I}$ lets intact our inflationary outputs, provided that Λ is determined by requiring $\Delta V_{\rm I}(\phi_\star) = 0$ or $\Delta V_{\rm I}(\phi_{\rm f}) = 0$. Namely, solving these conditions with respect to Λ we obtain

$$\Lambda = e^{c_m/c_\Lambda} \text{ with } \begin{cases} c_m = \widehat{m}_\theta^4 \ln \widehat{m}_\theta^2 + 2m_s^4 \ln m_s^2 - 4\widehat{m}_{\psi_\pm}^4 \ln \widehat{m}_{\psi_\pm}^2, \\ c_\Lambda = \widehat{m}_\theta^4 + 2m_s^4 - 4\widehat{m}_{\psi_\pm}^4. \end{cases} \tag{21}$$

If determined for $\phi = \phi_\star$ or $\phi = \phi_{\rm f}$, the expression above yields $\Lambda_\star = \Lambda(\phi_\star)$ or $\Lambda_{\rm f} = \Lambda(\phi_{\rm f})$. Both choices let intact the inflationary observables derived exclusively by using the (tree level) $V_{\rm I}$ in Equation (3) as shown for a similar model in Ref. [77]. Moreover, the renormalization-group running is expected to be negligible because Λ is close to the inflationary scale $H_{\rm I}$ (see below).

Table 1. Mass spectrum for CSI with $K = \widetilde{K}_{211\rm d}$ along the inflationary trajectory of Equation (13).

Fields	Eigenstates	Masses Squared/$H_{\rm I}^2$	
1 real scalar	$\widehat{\theta}$	$\widehat{m}_\theta^2/H_{\rm I}^2$	$3(n_{\rm d}(1-\phi)^2 + 4N\phi)/2N\phi \simeq 6$
2 real scalars	$s,\ \bar{s}$	$m_s^2/H_{\rm I}^2$	$6/N_S + 3n_{\rm d}^2(1-\phi)^2(nf_{\rm d} - n_{\rm d}\phi)^2/4N\phi^2$
2 Weyl spinors	$(\widehat{\psi}_\Phi \pm \widehat{\psi}_S)/\sqrt{2}$	$\widehat{m}_{\psi_\pm}^2/H_{\rm I}^2$	$3(1-\phi)^2(nf_{\rm d} - n_{\rm d}\phi)^2/8N\phi^2$

4. Gauge Non-Singlet Inflaton

In the present scheme, the inflaton field can be identified by the radial component of a conjugate pair of Higgs superfields. We here focus on the Higgs superfields, $\bar{\Phi}$ and Φ, which break the GUT symmetry $G_{\rm GUT} = G_{\rm SM} \times U(1)_X$ down to SM gauge group $G_{\rm SM}$ through their v.e.vs. We parameterize the involved superfields as follows

$$\Phi = \phi e^{i\theta}\cos\theta_\Phi \text{ and } \bar{\Phi} = \phi e^{i\bar{\theta}}\sin\theta_\Phi \text{ with } 0 \le \theta_\Phi \le \pi/2 \text{ and } S = (s + i\bar{s})/\sqrt{2}. \tag{22}$$

Note that superfield S is $G_{\rm GUT}$ singlet. As we verify in Section 4.3 below, a D-flat direction is

$$\langle\theta\rangle_{\rm I} = \langle\bar{\theta}\rangle_{\rm I} = 0,\ \langle\theta_\Phi\rangle_{\rm I} = \pi/4 \text{ and } \langle S\rangle_{\rm I} = 0, \tag{23}$$

which can be qualified as inflationary path. We below outline the SUGRA setting in Section 4.1 and determine the inflationary potential in Section 4.3 after canonically normalizing the various fields in Section 4.2. Finally, we give some information for the $U(1)_X$ phase transition in Section 4.4.

4.1. Setup

In accordance with our discussion in Section 2.2.2, we consider $F_{\rm W}$ as a function of the $G_{\rm GUT}$-invariant holomorphic quantity $\bar{\Phi}\Phi$, i.e.,

$$F_{\rm W} = (2\bar{\Phi}\Phi)^{n/4} - M^2 \text{ and so } W = \lambda S\Big((2\bar{\Phi}\Phi)^{n/4} - M^2\Big), \tag{24}$$

where λ and $M \ll 1$ are free parameters whereas n is a multiplier of 4. W is determined for $n = 4$ if we impose an R symmetry under which W has the charge of S whereas the

combination $\bar{\Phi}\Phi$ is uncharged. These two symmetries do not disallow, however, terms of the form $(\bar{\Phi}\Phi)^p$ with $p > 2$ in W and so stabilization of SI against corrections from those W terms dictates subplanckian values for $\bar{\Phi}$ and Φ or, via Equation (22), ϕ. On the other hand, for $n > 4$, the determination of W uniquely requires the imposition of an extra discrete symmetry $\mathbb{Z}_{n/4}$ under which $\bar{\Phi}\Phi$ has unit charge.

The realization of HSI can be accomplished by the consideration of two possible K's which are consistent with the imposed symmetries. They incorporate the following functions

$$F_{\rm sh} = 1 - 2\bar{\Phi}\Phi,\ F_{\rm d} = 1 + \sqrt{2\bar{\Phi}\Phi} \quad \text{and} \quad F_{\rm T} = \begin{cases} \left((1-2|\Phi|^2)(1-2|\bar{\Phi}|^2)\right)^{1/2} & \text{for } K = \widetilde{K}_{(11)^2}, \\ 1 - |\Phi|^2 - |\bar{\Phi}|^2 & \text{for } K = \widetilde{K}_{21}, \end{cases} \tag{25}$$

where the involved K's have been first introduced in ref. [66] and read

$$\widetilde{K}_{(11)^2} = -\frac{N}{2}\ln\frac{(1-2|\Phi|^2)(1-2|\bar{\Phi}|^2)}{(1-2\bar{\Phi}\Phi)(1-2\bar{\Phi}^*\Phi^*)} \quad \text{and} \quad \widetilde{K}_{21} = -N\ln\frac{1-|\Phi|^2-|\bar{\Phi}|^2}{\left((1-2\bar{\Phi}\Phi)(1-2\bar{\Phi}^*\Phi^*)\right)^{1/2}}. \tag{26}$$

These K's enjoy a shift symmetry, as shown in Appendix A, whose violation is expressed by

$$K_{\rm d} = -\frac{n_{\rm d}}{2}\ln(1+\sqrt{2\bar{\Phi}\Phi}) - \frac{n_{\rm d}}{2}\ln(1+\sqrt{2\bar{\Phi}^*\Phi^*}). \tag{27}$$

Therefore, the total K's for the two versions of HSI considered here are

$$\widetilde{K}_{2(11)^2{\rm d}} = K_2 + \widetilde{K}_{(11)^2} + K_{\rm d} \quad \text{and} \quad \widetilde{K}_{221{\rm d}} = K_2 + \widetilde{K}_{21} + K_{\rm d}, \tag{28}$$

where K_2 is given by Equation (5). These K's parameterize [66] the Kähler manifolds

$$\mathcal{M}_{2(11)^2} = \left(\frac{SU(2)}{U(1)}\right)_S \times \left(\frac{SU(1,1)}{U(1)}\right)^2_{\bar{\Phi}\Phi} \quad \text{or} \quad \mathcal{M}_{221} = \left(\frac{SU(2)}{U(1)}\right)_S \times \left(\frac{SU(2,1)}{SU(2)\times U(1)}\right)_{\bar{\Phi}\Phi}, \tag{29a}$$

with moduli-space scalar curvatures correspondingly [66]

$$\mathsf{R}_{2(11)^2} = -8/N + 2/N_S \quad \text{and} \quad \mathsf{R}_{221} = -6/N + 2/N_S. \tag{29b}$$

Note that in Equation (29a), we apply the same notation for the indices as in Equation (18).

4.2. Canonical Normalization

To obtain SI, we have to correctly identify the canonically normalized (hatted) fields of the $\bar{\Phi} - \Phi$ system, defined as follows:

$$\langle K_{\alpha\bar{\beta}}\rangle_{\rm I}\dot{z}^\alpha\dot{z}^{*\bar{\beta}} \simeq \frac{1}{2}\left(\dot{\hat{\phi}}^2 + \dot{\hat{\theta}}_+^2 + \dot{\hat{\theta}}_-^2 + \dot{\hat{\theta}}_\Phi^2\right), \tag{30}$$

where the elements $\langle K_{\alpha\bar{\beta}}\rangle_{\rm I}$ for the K's in Equation (26) are contained in the matrix $\mathbf{M}_{\bar{\Phi}\Phi}$ (see Equation (A1) of Appendix A) whose form in the limit of Equation (23) is

$$\langle \mathbf{M}_{\bar{\Phi}\Phi}\rangle_{\rm I} = \begin{cases} \kappa\,\mathsf{diag}(1,1) & \text{for } K = \widetilde{K}_{(11)^2}, \\ \kappa\begin{pmatrix} 1-\phi^2/2 & \phi^2/2 \\ \phi^2/2 & 1-\phi^2/2 \end{pmatrix} & \text{for } K = \widetilde{K}_{21}, \end{cases} \quad \text{with } \kappa = N/f_{\rm T}^2. \tag{31}$$

Expanding the second term of the right-hand side of Equation (4a) along the path in Equation (13) for $\alpha = \bar{\Phi}, \Phi$ and substituting Equation (31), we obtain

$$\langle K_{\alpha\bar{\beta}}\rangle_{\rm I}\dot{z}^{\alpha}\dot{z}^{*\bar{\beta}} = \begin{cases} \kappa\dot{\phi}^2 + \kappa\phi^2\left(\dot{\theta}_+^2 + \dot{\theta}_-^2 + 2\dot{\theta}_\Phi^2\right)/2 & \text{for} \quad K = \widetilde{K}_{(11)^2}, \\ \kappa_+\left(\dot{\phi}^2 + \phi^2\dot{\theta}_+^2/2\right) + \kappa_-\phi^2\left(\dot{\theta}_-^2/2 + \dot{\theta}_\Phi^2\right) & \text{for} \quad K = \widetilde{K}_{21}, \end{cases} \tag{32a}$$

with $\kappa_+ = \kappa$, $\kappa_- = \kappa f_{\rm T}$ and $\theta_\pm = \left(\bar{\theta} \pm \theta\right)/\sqrt{2}$. Comparing Equations (30) and (32a), we can derive the relation between the hatted and unhatted fields. Regarding the inflaton, the equality between κ and κ_+ in Equation (32a) assures that, for both K's, the $d\widehat{\phi}/d\phi$ relation is identical with that found in Equation (19) and so the correct $\phi - \widehat{\phi}$ relation in Equation (2) emerges. For the remaining fields of the $\bar{\Phi} - \Phi$ system, we find

$$\begin{aligned} &\widehat{\theta}_\pm = \sqrt{\kappa}\phi\theta_\pm, \ \widehat{\theta}_\Phi = \sqrt{2\kappa}\phi(\theta_\Phi - \pi/4) && \text{for} \quad K = \widetilde{K}_{(11)^2}, \\ &\widehat{\theta}_+ = \sqrt{\kappa_+}\phi\theta_+, \ \widehat{\theta}_- = \sqrt{\kappa_-}\phi\theta_-, \ \widehat{\theta}_\Phi = \sqrt{2\kappa_-}\phi(\theta_\Phi - \pi/4) && \text{for} \quad K = \widetilde{K}_{21}, \end{aligned} \tag{32b}$$

where we take into account that the masses of the scalars other than $\widehat{\phi}$ during SI are large enough such that the dependence of the hatted fields on ϕ does not influence their dynamics. Needless to say, the extra contributions into the K's in Equation (26) do not disturb our formulae above.

4.3. Inflationary Potential

Upon substitution of W and K from Equations (24) and (26) into Equation (6) we arrive at the advertised form of $V_{\rm I}$ in Equation (3). With regard to $V_{\rm D}$ (see Equation (4d)) for the K's in Equation (26), D_X takes the form

$$\mathrm{D}_X = N\Big(|\Phi|^2 - |\bar{\Phi}|^2\Big) \cdot \begin{cases} (1 - 2|\bar{\Phi}|^2)^{-1}(1 - 2|\Phi|^2)^{-1} & \text{for} \quad K = \widetilde{K}_{2(11)^2\mathrm{d}}, \\ \left(1 - |\Phi|^2 - |\bar{\Phi}|^2\right)^{-1} & \text{for} \quad K = \widetilde{K}_{221\mathrm{d}}\,. \end{cases} \tag{33}$$

If we insert this result into Equation (4d) and take the limit of Equation (23), we deduce that $\langle V_{\rm D}\rangle_{\rm I} = 0$ and so no D-term contribution arises in $V_{\rm SUGRA}$ during HSI.

We can also proceed in deriving the mass spectrum of the models along the direction of Equation (23) and verifying its stability against the fluctuations of the non-inflaton fields. The results of our computation are accumulated in Table 2. As for spectrum in Table 1, $N_S < 6$ plays a crucial role in retaining positive and heavy enough $\widehat{m}_s^2$ whereas $\widehat{\theta}_+$ turns out to be spontaneously heavy enough as $\widehat{\theta}$ in Table 2. Here, however, we also display the masses, of $\widehat{\theta}_\Phi$, of the gauge boson A_X and of the corresponding fermions which acquire contribution from the gauge sector of the theory, and so they are safely heavy and stabilized. The unspecified eigenstate $\widehat{\psi}_\pm$ is defined as

$$\widehat{\psi}_\pm = (\widehat{\psi}_{\Phi+} \pm \psi_S)/\sqrt{2} \ \text{ where } \ \psi_{\Phi\pm} = (\psi_{\bar{\Phi}} \pm \psi_\Phi)/\sqrt{2} \tag{34}$$

with the spinors ψ_S and $\psi_{\Phi\pm}$ being associated with the superfields S and $\bar{\Phi} - \Phi$. Comparing the various masses we notice only minor discriminations between the two analyzed K's.

The non-zero M_X signals the fact that $U(1)_X$ is broken during SI since A_X becomes massive absorbing the massless Goldstone boson associated with $\widehat{\theta}_-$. As a consequence, six degrees of freedom before the spontaneous breaking (four corresponding to the two complex scalars $\bar{\Phi}$ and Φ and two corresponding to the massless gauge boson A_X of $U(1)_X$) are redistributed as follows: three degrees of freedom are associated with the real propagating scalars ($\widehat{\theta}_+$, $\widehat{\theta}_\Phi$ and $\widehat{\phi}$), whereas the residual one degree of freedom combines together with the two ones of the initially massless gauge boson A_X to make it massive. From Table 2, we can also deduce that the numbers of bosonic (eight) and fermionic (eight) degrees of freedom are equal if we take into account the inflaton ϕ not included.

The derived mass spectrum allows us to determine the one-loop radiative corrections to $V_{\rm I}$ employing the Coleman–Weinberg formula (see, e.g., ref. [77]). However, we remark that $M_{\rm X}^2 \gg m_{\rm P}^2$ and $\widehat{m}_{\theta_\Phi}^2 \gg m_{\rm P}^2$, and so these masses cannot be included in the formula above [77]. As a consequence, $\Delta V_{\rm I}$ and $\Lambda_\star$ assume the same expressions as in Equations (20) and (21), respectively, with the relevant masses replaced by those defined in Table 2.

Table 2. Mass spectrum for HSI along the inflationary trajectory of Equation (23).

Fields	**Eigen-states**		**Masses Squared**	
			$K = \widetilde{K}_{\mathbf{2(11)^2d}}$	$K = \widetilde{K}_{\mathbf{221d}}$
4	$\widehat{\theta}_+$	$m_{\widehat{\theta}+}^2$	$3H_{\rm I}^2(n_{\rm d}(1-\phi)^2+4N\phi)/4N\phi \simeq 3H_{\rm I}^2$	
real	$\widehat{\theta}_\Phi$	$\widehat{m}_{\theta_\Phi}^2$	$M_{\rm X}^2+6H_{\rm I}^2-3H_{\rm I}^2\cdot$	$M_{\rm X}^2+6H_{\rm I}^2-3H_{\rm I}^2\cdot$
scalars			$(1-\phi)^2 f_{\rm d}(nf_{\rm d}-n_{\rm d}\phi)/N\phi^2$	$(1-\phi)(nf_{\rm d}-n_{\rm d}\phi)/N\phi^2$
	$s,\bar{s}$	$\widehat{m}_s^2$	$H_{\rm I}^2(6/N_S+3(1-\phi)^2(nf_{\rm d}-n_{\rm d}\phi)^2/N\phi^2)$	
1 gauge boson	A_X	$M_{\rm X}^2$	$2Ng^2\phi^2/f_{\rm T}^2$	$2Ng^2\phi^2/f_{\rm T}$
4 Weyl	$\widehat{\psi}_\pm$	$\widehat{m}_{\psi\pm}^2$	$3(1-\phi)^2(nf_{\rm d}-n_{\rm d}\phi)^2H_{\rm I}^2/8N\phi^2$	
spinors	$\lambda_X, \widehat{\psi}_{\Phi-}$	$M_{\rm X}^2$	$2Ng^2\phi^2/f_{\rm T}^2$	$2Ng^2\phi^2/f_{\rm T}$

4.4. $U(1)_X$ Phase Transition

In the context of HSI, W in Equation (24) leads not only to an inflationary era but also to the breaking of $U(1)_X$ symmetry. In our introductory setup the v.e.vs. of $\bar{\Phi}$ and Φ break $U(1)_X$ down to $\mathbb{Z}_2^X$. Indeed, minimizing $V_{\rm I}$ in Equation (3) with $\phi \ll m_{\rm P}$, we find that a SUSY vacuum arises after the end of HSI determined as follows:

$$\langle S\rangle = 0 \;\text{ and }\; |\langle 2\bar{\Phi}\Phi\rangle|^{n/4} = M^2 \;\Rightarrow\; \langle\phi\rangle = M^{4/n}. \tag{35}$$

Although $\langle\Phi\rangle$ and $\langle\bar{\Phi}\rangle$ break spontaneously $U(1)_X$, no cosmic strings are produced at the SUSY vacuum, since this symmetry is already broken during HSI (cf. ref. [85]). The contributions from the soft SUSY breaking terms can be safely neglected within contemporary SUSY, since the corresponding mass scale is much smaller than M. They may shift [31,36,48,68,85], however, slightly $\langle S\rangle$ from zero in Equation (35).

Regarding the value of M, it can be determined by requiring that $\langle\bar{\Phi}\Phi\rangle$ takes the value dictated by the unification of MSSM gauge coupling constants. In particular, the unification scale $M_{\rm GUT} \simeq 2/2.433\times 10^{-2} \simeq 8.22\cdot 10^{-3}$ is to be identified with $\langle M_{\rm X}\rangle$ (see Table 2), i.e.,

$$\langle M_{\rm X}\rangle = \sqrt{2N}gM \simeq M_{\rm GUT} \;\Rightarrow\; M \simeq \left(M_{\rm GUT}/g\sqrt{2N}\right)^{n/4} \;\text{ for }\; \langle f_{\rm T}\rangle \simeq 1. \tag{36}$$

Here, $g \simeq 0.7$ is the value of the GUT gauge coupling constant.

The determination of M influences heavily the inflaton mass at the vacuum, $\widehat{m}_{\rm I}$ and induces an N dependence in the results. Indeed, the (canonically normalized) inflaton,

$$\widehat{\delta\phi} = \langle J\rangle\delta\phi \;\text{ with }\; \delta\phi = \phi - \langle\phi\rangle \;\text{ and }\; \langle J\rangle = \sqrt{2N}/\langle f_{\rm T}\rangle \tag{37}$$

acquires mass, at the SUSY vacuum in Equation (35), which is given by

$$\widehat{m}_{\rm I} = \left\langle V_{{\rm I},\widehat{\phi}\widehat{\phi}}\right\rangle^{1/2} = \left\langle V_{{\rm I},\phi\phi}/J^2\right\rangle^{1/2} = \frac{\lambda n M^{2(1-2/n)}}{2\sqrt{N}}\frac{1-M^{8/n}}{\left(1+M^{4/n}\right)^{n_{\rm d}/2}}. \tag{38}$$

Since $M \ll m_{\rm P}$, this result is essentially valid for both K's in Equation (26). Note in passing that the mass of the inflaton for CSI with $n=2$ is given by $\widehat{m}_{\rm I} = \sqrt{2/N}\lambda m_{\rm P}$.

5. Inflation Analysis

We proceed now to the analytic and numeric investigation of the viability of our models in Sections 5.1 and 5.2.

5.1. Analytic Results

Since both models (CSI and HSI) are based on the same $\phi - \widehat{\phi}$ relation in Equation (2) and the same $V_{\rm I}$ in Equation (3), their analysis can be performed in a unified way. Namely, the period of slow-roll SI is determined by the condition (see, e.g., refs. [2,4]):

$$\max\{\epsilon(\widehat{\phi}), |\eta(\widehat{\phi})|\} \simeq 1, \text{ where } \epsilon = \frac{1}{2}\left(\frac{V_{\rm I,\widehat{\phi}}}{V_{\rm I}}\right)^2 \text{ and } \eta = \frac{V_{\rm I,\widehat{\phi}\widehat{\phi}}}{V_{\rm I}} \tag{39a}$$

are the slow-roll parameters which and can be estimated employing J in Equation (19) without express explicitly $V_{\rm I}$ in terms of $\widehat{\phi}$. Indeed, our results are found to be

$$\epsilon = \frac{(\phi-1)^2(nf_{\rm d} - n_{\rm d}\phi)^2}{2N\phi^2} \quad \text{and} \quad \eta = \frac{(\phi-1)}{N\phi^2}\cdot$$
$$\Big(n^2(\phi-1)f_{\rm d}^2 + n\Big((1-2n_{\rm d})\phi^3 + 2n_{\rm d}\phi + \phi^2 + f_{\rm d}\Big) + n_{\rm d}\phi^2(n_{\rm d}(\phi-1) - f_{\rm d})\Big). \tag{39b}$$

Equation (39a) is saturated for $\phi = \phi_{\rm f}$, which is the maximal values from the following two solutions

$$\phi_{1\rm f} \simeq \frac{\sqrt{4.n^2 + 2nN - 4nn_{\rm d} + n_{\rm d}^2} - n_{\rm d}}{2(2n + N - 2n_{\rm d})}; \tag{40a}$$

$$\phi_{2\rm f} \simeq \frac{\sqrt{4n^2n_{\rm d}^2 - 4n(n-1)(-n^2 + 2nn_{\rm d} + n + N)} + 2nn_{\rm d}}{2(2n - n^2 + n_{\rm d} + n + N)}\cdot \tag{40b}$$

In practice, for $n_{\rm d} < n/2$, $\phi_{1\rm f} < \phi_{2\rm f}$ and so SI terminates at $\phi_{\rm f} = \phi_{2\rm f}$ whereas larger $n_{\rm d}$'s give rise to the inverse hierarchy and so $\phi_{\rm f} = \phi_{1\rm f}$.

The number of e-foldings $N_\star$ that the pivot scale $k_\star = 0.05/\text{Mpc}$ experiences during SI is estimated as

$$N_\star = \int_{\widehat{\phi}_{\rm f}}^{\widehat{\phi}_*} d\widehat{\phi}\frac{V_{\rm I}}{V_{\rm I,\widehat{\phi}}} = N(I_N(\phi_\star) - I_N(\phi_{\rm f})), \tag{41}$$

where $\widehat{\phi}_*$ and $\phi_\star$ are the values of $\widehat{\phi}$ and ϕ, respectively, when $k_\star$ crosses outside the inflationary horizon, and the involved function I_N reads

$$I_N(\phi) = \frac{n_{\rm d}}{4\delta n^2}\ln(1-\phi) - \frac{1}{2\delta n(1-\phi)} - \frac{1}{4n_{\rm d}}\ln f_{\rm d} + \frac{n(n-n_{\rm d})}{n_{\rm d}\delta n^2}\ln(nf_{\rm T} - n_{\rm d}\phi), \tag{42}$$

where $\delta n = n_{\rm d} - 2n < 0$. The last inequality stems from the fact that the dominant contribution to I_N originates from the non-logarithmic term with $\phi < 1$. The presence of a pole in J (see Equation (19)) and the effective nature of SUGRA forces us to work in this domain of ϕ. Consequently, the positivity of $N_\star$ implies the upper bound above on δn which restricts seriously the allowed region of our model as we see in Section 5.2.

Due to the complicate form of $N_\star$ in Equation (41), it is not doable to solve the equation above with respect to $\phi_\star$ and find a generic analytical expression for it and the inflationary observables (see below). As a consequence, our last resort is a numerical computation, whose results are presented in Section 5.2. Nonetheless, for $n_{\rm d} \ll n$ and taking into account $\phi_\star \gg \phi_{\rm f}$, we can derive an approximate and rather accurate formula for $N_\star$ since it is

dominated from the non-logarithmic term of I_N. In this portion of parameter space, we can determine $\phi_\star$ as follows

$$N_\star \simeq -\frac{N}{2\delta n}\frac{\phi_\star}{1-\phi_\star} \;\Rightarrow\; \phi_\star \simeq \frac{2\delta n N_\star}{2\delta n N_\star - N}. \tag{43}$$

Since both factors of the ratio above are negative, and the denominator is larger in absolute value we expect that $\phi_\star < 1$. Therefore, our proposal can be stabilized against corrections from higher-order terms in the K's (see Section 4.2).

The amplitude A_s of the power spectrum of the curvature perturbations generated by ϕ can be computed using the standard formulae

$$A_\mathrm{s}^{1/2} = \frac{1}{2\sqrt{3}\,\pi}\frac{V_\mathrm{I}^{3/2}(\widehat{\phi}_*)}{|V_{\mathrm{I},\widehat{\phi}}(\widehat{\phi}_*)|} = \frac{\lambda\phi_\star\sqrt{N}\sqrt{\phi_\star^n(1+\phi_\star)^{-n_\mathrm{d}}}}{2\sqrt{3}\pi(1-\phi_\star)(nf_{\mathrm{T}\star}-n_\mathrm{d}\phi_\star)}, \tag{44}$$

where $f_{\mathrm{T}\star} = f_\mathrm{T}(\phi_\star)$. From the right formula in Equation (44), we can derive a relation between λ and A_s. For simplicitly, we set $n_\mathrm{d} = 0$, and so we find

$$\lambda \simeq \frac{\pi n^{-\frac{n}{2}}\sqrt{3A_\mathrm{s}}\sqrt{N}(8nN_\star+N)}{2^{n+1}N_\star^{\frac{n}{2}+1}(4nN_\star+N)^{1-n/2}}. \tag{45}$$

It is clear that no δn dependence appears due to the drastic simplification. However, the numerical result is quite close to the exact one given that n_d is bounded above as noticed from Equation (42).

The remaining inflationary observables—i.e., the (scalar) spectral index n_s, its running a_s, and the scalar-to-tensor ratio r—are found from the relations [2,4]

$$n_\mathrm{s} = 1 - 6\epsilon_\star + 2\eta_\star,\; r = 16\epsilon_\star \;\text{ and }\; \alpha_\mathrm{s} = 2\Big(4\eta_\star^2 - (n_\mathrm{s}-1)^2\Big)/3 - 2\widehat{\xi}_\star, \tag{46}$$

where the variables with subscript $\star$ are evaluated at $\phi = \phi_\star$ and $\widehat{\xi} = V_{\mathrm{I},\widehat{\phi}}V_{\mathrm{I},\widehat{\phi}\widehat{\phi}\widehat{\phi}}/V_\mathrm{I}^2$. Inserting $\phi_\star$ from Equations (43) into (39b) and then into equations above, we can obtain the following approximate expressions

$$n_\mathrm{s} \simeq 1 - \frac{2}{N_\star} - \frac{n_\mathrm{d}^2 N}{4N_\star^2\delta n^2} - \frac{n^2 N}{N_\star^2\delta n^2} + \frac{n_\mathrm{d} n N}{N_\star^2\delta n^2} - \frac{3n_\mathrm{d}N}{2N_\star^2\delta n^2} + \frac{nN}{N_\star^2\delta n^2}, \tag{47a}$$

$$r \simeq \frac{2N}{N_\star^2} + \frac{2n_\mathrm{d}N^2}{N_\star^3\delta n^2} - \frac{2nN^2}{N_\star^3\delta n^2}, \tag{47b}$$

$$\alpha_\mathrm{s} \simeq -\frac{2}{N_\star^2} - \frac{n_\mathrm{d}^2 N}{2N_\star^3\delta n^2} - \frac{2n^2 N}{N_\star^3\delta n^2} + \frac{2n_\mathrm{d} n N}{N_\star^3\delta n^2} - \frac{7n_\mathrm{d}N}{2N_\star^3\delta n^2} + \frac{2nN}{N_\star^3\delta n^2}. \tag{47c}$$

These expressions give accurate results for $n_\mathrm{d} \ll n$ or $\delta n \simeq -2n$. For $n = n_\mathrm{d} = 2$, the above results converge to those obtained for the pure α-SI [20,57,61,62], i.e.,

$$(n_\mathrm{s}, r, \alpha_\mathrm{s}) \simeq (1 - 2/N_\star, 2N/N_\star^2, -2/N_\star^2). \tag{48}$$

The same results are obtained (for reasonably low n and N values) in the limit $n_\mathrm{d} = 0$ where the pure T-model inflation is revealed.

5.2. Numerical Results

Our estimations above can be verified and extended for any δn numerically. In particular, we confront the quantities in Equations (41) and (44) with the observational requirements [87]

$$N_\star \simeq 61.3 + \frac{1-3w_{\rm rh}}{12(1+w_{\rm rh})}\ln\frac{\pi^2 g_{\rm rh*}T_{\rm rh}^4}{30V_{\rm I}(\phi_{\rm f})} + \frac{1}{2}\ln\left(\frac{V_{\rm I}(\phi_\star)}{g_{\rm rh*}^{1/6}V_{\rm I}(\phi_{\rm f})^{1/2}}\right) \quad \text{and} \quad A_{\rm s}^{1/2} \simeq 4.588\cdot 10^{-5}, \tag{49}$$

where we assume that SI is followed in turn by an oscillatory phase with mean equation-of-state parameter $w_{\rm rh}$, radiation and matter domination. Motivated by implementations [31,36,37,68] of non-thermal leptogenesis, which may follow SI, we set $T_{\rm rh} \simeq 1$ EeV for the reheat temperature. Also, we take for the energy-density effective number of degrees of freedom $g_{\rm rh*} = 228.75$ which corresponds to the MSSM spectrum. Note that this $T_{\rm rh}$ avoids exhaustive tuning on the relevant coupling constant involved in the decay width of the inflaton (refs. [62,83]).

Due to the peculiar expression of $V_{\rm I}$ in Equation (3) and the non-minimal kinetic mixing in Equation (2), the estimation of $w_{\rm rh}$ requires some care (refs. [88–90]). We determine it adapting the general formula [91], i.e.,

$$w_{\rm rh} = 2\frac{\int_{\phi_{\rm mn}}^{\phi_{\rm mx}} d\phi J(1-V_{\rm I}/V_{\rm I}(\phi_{\rm mx}))^{1/2}}{\int_{\phi_{\rm mn}}^{\phi_{\rm mx}} d\phi J(1-V_{\rm I}/V_{\rm I}(\phi_{\rm mx}))^{-1/2}} - 1, \tag{50}$$

where $\phi_{\rm mn} = 0$ for CSI whereas $\phi_{\rm mn} = \langle\phi\rangle$ given in Equation (35) for HSI. The amplitude of the oscillations during reheating $\phi_{\rm mx}$ is found by solving numerically the condition $\sqrt{3}H_{\rm I}(\phi_{\rm mx}) = \widehat{m}_{\rm I}$ if $\widehat{m}_{\rm I} < \sqrt{3}H_{\rm I}(\phi_{\rm f})$ or it is $\phi_{\rm mx} = \phi_{\rm f}$ otherwise. The result deviates slightly from the naive expectation according to which

$$w_{\rm rh} = (n-2)/(n+2), \tag{51}$$

for a monomial power-law potential of the form ϕ^n.

Enforcing Equation (49), we can restrict λ and $\phi_\star$ via Equation (41). In general, we obtain $\lambda \sim 10^{-5}$ in agreement with Equation (45). Regarding $\phi_\star$, we assume that ϕ starts its slow roll below the location of kinetic pole, i.e., $\phi = 1$, consistently with our approach to SUGRA as an effective theory below $m_{\rm P} = 1$. The closer to the pole that $\phi_\star$ is set, the larger the value of $N_\star$ that is obtained. Therefore, a tuning of the initial conditions is required, which can be somehow quantified defining the quantity

$$\Delta_\star = (1-\phi_\star). \tag{52}$$

The naturalness of the attainment of SI increases with $\Delta_\star$. After the extraction of λ and $\phi_\star$, we compute the models' predictions via Equation (46), for any selected values for the remaining parameters, N, n and $n_{\rm d}$, with $M \ll 1$. Our outputs are encoded as lines in the $n_{\rm s} - r$ plane and compared against the observational data [92]. We take into account the latest *Planck release 4* (PR4) including TT, TE, EE+lowE power spectra [93], *Baryon Acoustic Oscillations* (BAO), CMB-lensing and BICEP/*Keck* (BK18) data. Fitting it [92] with ΛCDM, we obtain the marginalized joint 68% [95%] regions depicted by the dark [light] shaded contours in the aforementioned figures. Approximately, we obtain

$$\text{(a)}\ \ n_{\rm s} = 0.965 \pm 0.009 \quad \text{and} \quad \text{(b)}\ \ r \lesssim 0.032 \tag{53}$$

at a 95% *confidence level* (c.l.) with negligible $\alpha_{\rm s}$ (cf. Ref. [62]). The results are exposed separately in Sections 5.2.1 and 5.2.2 for CSI and HSI, respectively.

5.2.1. SI with a Gauge-Singlet Inflaton (CSI)

In this case, we consider throughout $n = 2$ which is motivated by the quadratic potential which is usually encountered for gauge-singlet superfields. The comparison of the model predictions with data is displayed in Figure 1, where we plot r versus $n_{\rm s}$ for $n_{\rm d} = 1$ (dashed line), $n_{\rm d} = 2$ (solid line) or $n_{\rm d} = 3$ (dot-dashed line). The variation in N is given along each curve. We observe that the whole observationally favored range of r is covered varying N whereas $n_{\rm s}$ remains close to its central value in Equation (53). As a consequence, an upper bound on N can be derived. This bound increases with $n_{\rm d}$. Varying continuously N from 1 until that maximal value, derived from the upper bound on r in Equation (53b), we obtain the shaded region in Figure 2. That upper bound, indicated by a dashed line, in conjunction with the upper bound on $n_{\rm d}$ inferred by Equation (42) and depicted by a solid line, delineate clearly the allowed (shaded) parameter space of our model. In all, we find

$$1 \lesssim N \lesssim 180, \quad 0 \leq n_{\rm d} \leq 3.99, \quad 0.961 \lesssim n_{\rm s} \lesssim 0.966 \quad \text{and} \quad 1 \lesssim \Delta_\star/100 \lesssim 53 \tag{54a}$$

with $w_{\rm rh} \simeq 0$, $\alpha_{\rm s} \simeq -(6.5 - 7.5) \cdot 10^{-4}$ and $N_\star \simeq (50 - 52)$. It is impressive that the $\Delta_\star$ values are much larger than the values derived in T-model Higgs inflation analyzed in refs. [54,66,85], and therefore the present model can be characterized as more natural. Note that the naturalness of the model further requests $n_{\rm d} \ll N$ since in this regime the 't Hooft argument [69] is more well suited. Moreover, λ and $\widehat{m}_{\rm I}$ range as follows

$$3.6 \cdot 10^{-5} \lesssim \lambda \lesssim 1.4 \cdot 10^{-4} \quad \text{and} \quad 1.6 \lesssim \widehat{m}_{\rm I}/10 \text{ ZeV} \lesssim 4.7. \tag{54b}$$

The maximal $\widehat{m}_{\rm I}$ values are obtained for the largest $n_{\rm d}$ and the minimal N, as deduced from the expression shown below Equation (38).

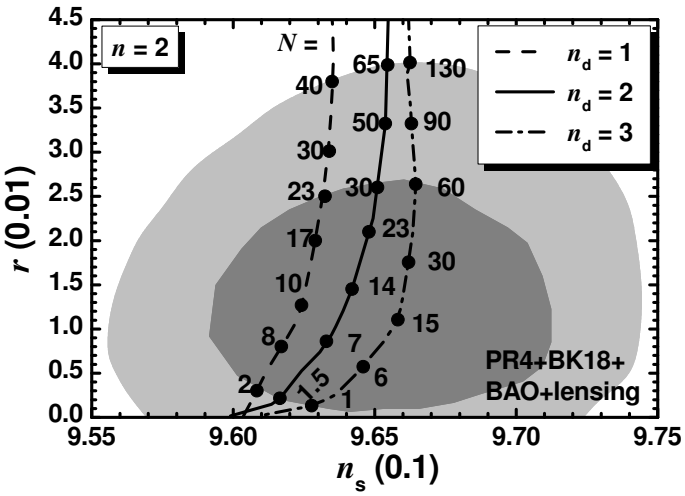

Figure 1. Curves allowed by Equation (49) in the $n_{\rm s} - r$ plane for CSI with $n = 2$, various N's indicated along them and $n_{\rm d} = 1$ (dashed line), $n_{\rm d} = 2$ (solid line), or $n_{\rm d} = 3$ (dot-dashed line). The marginalized joint 68% [95%] c.l. regions [92] from PR4, BK18, BAO and lensing datasets are depicted by the dark [light] shaded contours.

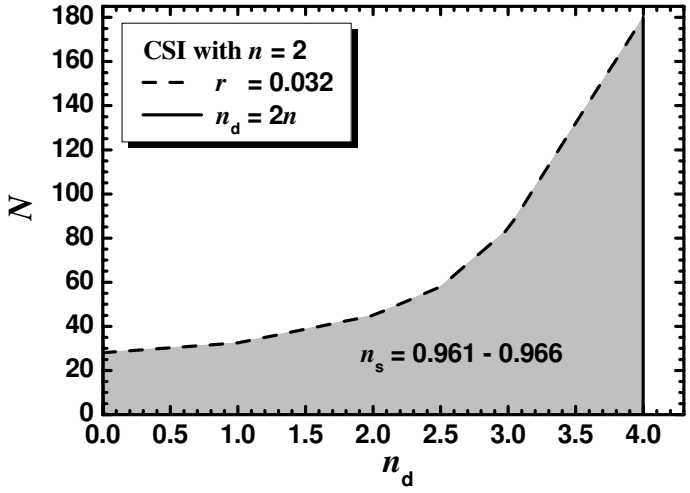

Figure 2. Allowed (shaded) region as determined by Equations (49) and (53) in the $n_{\rm d} - N$ plane for CSI with $n = 2$. The conventions adopted for the boundary curves are also shown.

Representative values of model parameters, field values, and observables are given in the two leftmost columns of Table 3 for $N = 10$. This N value gives a value for $(n_{\rm s}, r)$ in the current "sweet" spot of the dark shaded region in Figure 1. We notice the following: (i) $\phi_\star$ and $\phi_{\rm f}$ are subplanckian in accordance with the consideration of SUGRA as an effective theory below $m_{\rm P} = 1$; (ii) $\Delta_\star$ increases with $n_{\rm d}$; (iii) λ acquires a soft dependence from $n_{\rm d}$ not shown in its analytical expression in Equation (45); (iv) $\Lambda_\star < m_{\rm P}$ is quite close to $H_{{\rm I}\star}$ and so the effects of the renormalization group running are negligible; (v) $w_{\rm rh}$ estimated by Equation (50) is a little lower than its naive value obtained by Equation (51); and (vi) the values derived from the analytical expressions of Section 5.1 and written in italics are quite reliable for $n_{\rm d} = 1$.

Table 3. Parameters, field values, and observables allowed by Equations (49) and (53) for CSI with $n = 2$ and HSI with $\langle M_{\rm X} \rangle = M_{\rm GUT}$ and (i) $n = 4$ or (ii) $n = 8$. In all cases, we take $N = 10$. Values in square brackets are obtained from our analytical expressions in Section 5.1.

Model:	**CSI**		**HSI**		**HSI**	
n	2		4		8	
$n_{\rm d}$	1	3	1	7	1	15
$\phi_\star/0.1m_{\rm P}$	9.43 {*9.4*}	8.8	9.76 {*9.7*}	9.1	9.7 {*9.9*}	9.4
$\Delta_\star(\%)$	5.7	11.5	2.4	9	1.5	7
$\phi_{\rm f}/0.1m_{\rm P}$	2.6 {*1.9*}	2.2	4.7 {*2.6*}	3.2	6.9 {*3.3*}	4.4
$w_{\rm rh}$	−0.065	−0.14	0.29	0.27	0.5	0.49
$N_\star$	51.5 {*55*}	50.9	56.5 {*58*}	55.4	58.8 {*60*}	58.1
$\lambda/10^{-5}$	2.9 {*2.2*}	4.7	2.8	16.3	2.7	23.2
$\Lambda_\star/10^{-5}m_{\rm P}$	2.3	2.8	2.6	1.6	2.5	1.7
$H_{{\rm I}\star}/10^{-5}m_{\rm P}$	1.1	0.93	1.1	0.81	1.1	0.72
$n_{\rm s}/0.1$	9.62 {*9.6*}	9.65	9.64 {*9.63*}	9.67	9.66 {*9.65*}	9.68
$-\alpha_{\rm s}/10^{-4}$	7.1 {*8.2*}	6.6	6.3 {*6.7*}	5.8	5.8 {*6.2*}	5.9
$r/10^{-2}$	1.3 {*1.4*}	0.8	1.1 {*1.2*}	0.63	1.1 {*1.1*}	0.05
M	–		6.4 YeV		16.8 ZeV	
$\widehat{m}_{\rm I}$	22.6 ZeV	36.4 ZeV	79.7 EeV	46 EeV	1.1 PeV	89.6 PeV

5.2.2. SI with a Higgs Field (HSI)

In this case, we consider two representative values, $n = 4$ and $n = 8$, which are appropriate for the self-consistency of W in Equation (24). We also fix M throughout, imposing the GUT condition in Equation (36). Since this is indistinguishable for both K's considered in Section 4.2, our results are identical for both cases. However, our results are valid for any other M value provided that $M \ll m_{\rm P}$.

Several characteristic inputs and outputs for HSI with the aforementioned n values are listed in the central and the rightmost columns of Table 3. We take $N = 10$ and $n_{\rm d} = 1$ and $n_{\rm d} = 2n - 1$ for both selected n values. Recall that viable HSI requires $n_{\rm d} < 2n$ (see Equations (41) and (42)). The remarks in the end of Section 5.2.1 regarding the findings of Table 3 are valid for HSI. Nonetheless, in this case we also present the M and $\widehat{m}_{\rm I}$ values that are estimated via Equations (36) and (38), respectively. We see that both mass parameters decrease as n increases and only $\widehat{m}_{\rm I}$ develops a dependence on $n_{\rm d}$ as expected from the equations above.

One notable feature of our proposal is the fact that SI replaces subplanckian ϕ values. The naive assessment that this achievement is not consistent with the chaotic character of SI is not appropriate since ϕ does not coincide with the canonically normalized inflaton, $\widehat{\phi}$. If we take into account the $\phi - \widehat{\phi}$ relation of Equation (2), we can easily infer that $\widehat{\phi}$ acquires transplanckian values for $\phi < 1$ and so SI is rendered feasible (cf. refs. [10,31–33,35,36,54,66]). To further clarify this key feature of our models, we comparatively plot $V_{\rm I}$ in Equation (3) as a function of ϕ in Figure 3a and $\widehat{\phi}$ in Figure 3b for $N = 10$, $n = 4$ and $n_{\rm d} = 1$ (black lines) and $n_{\rm d} = 7$ (gray lines).

From Figure 3a, we see that $V_{\rm I}$ for both $n_{\rm d}$ values has a parabolic-like slope for $\phi < 1$. On the contrary, in Figure 3b $V_{\rm I}$ experiences a stretching for $\widehat{\phi} > 1$ which results to the well-known plateau of SI for $\widehat{\phi} \gg 1$ (see, e.g., Ref. [10]). The observationally relevant inflationary period is limited between the two ϕ values $\phi_{\rm f}$ and $\phi_\star$ which are given in the two middle columns of Table 3 and are depicted in Figure 3a. These values are enhanced, as advocated above, and indicated in Figure 3b. Namely, solving Equation (2) with respect to $\widehat{\phi}$, we can estimate $\widehat{\phi}_{\rm f} = 2.3$ and $\widehat{\phi}_* = 9.9$ for $n_{\rm d} = 1$ and $\widehat{\phi}_{\rm f} = 1.5$ and $\widehat{\phi}_* = 6.8$ for $n_{\rm d} = 7$. Also shown in the inset of Figure 3a is the structure of $V_{\rm I}$ for low ϕ values responsible for the implementation of the $U(1)_X$ phase transition (see Section 4.4).

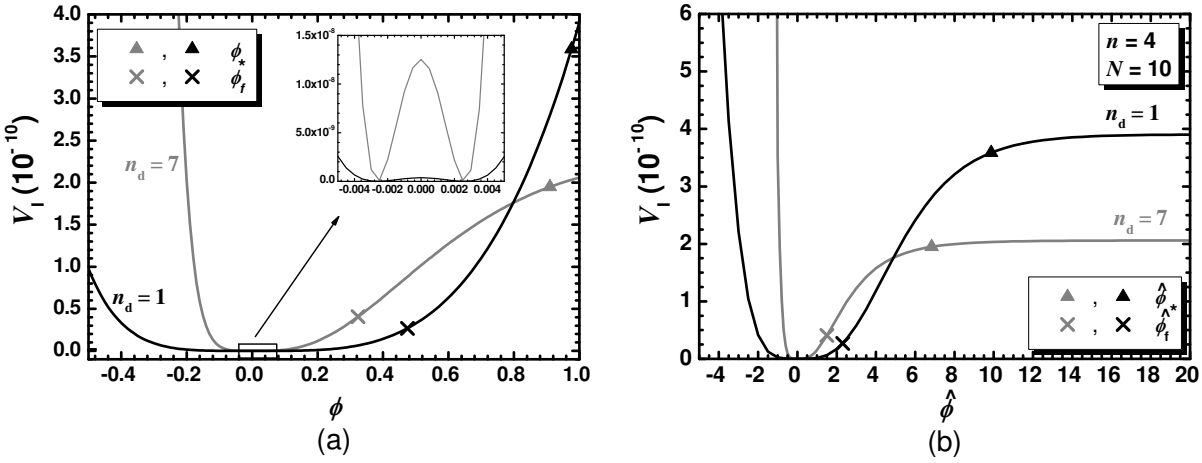

Figure 3. Inflationary potential $V_{\rm I}$ as a function of (**a**) ϕ and (**b**) $\widehat{\phi}$ fixing $\langle M_X \rangle = M_{\rm GUT}$. We consider HSI with $N = 10$, $n = 4$ and $n_{\rm d} = 1$ (black lines) or $n_{\rm d} = 7$ (gray lines). Values corresponding to $\phi_\star$ and $\phi_{\rm f}$ (**a**) or $\widehat{\phi}$ and $\widehat{\phi}_{\rm f}$ (**b**) are depicted. Shown also is the low-ϕ behavior of $V_{\rm I}$ in the inset (**a**).

From Figure 3b, we remark that for both $n_{\rm d}$ values the magnitudes of the two plateaus are of the order 10^{-10} which are similar to that obtained in pure SI [10,31,32,36,37,48,49,58].

However, these are one order lower than obtained in ref. [33], where r is a little more enhanced. Indeed, as verified from the values listed in Table 3, the level of the inflationary plateau increases with r. Moreover, the inflationary scale $V_{\rm I}^{1/4}$ turns out to be well below $m_{\rm P}$, and so the semi-classical approximation, used in our analysis, is perfectly valid. Note that here $m_{\rm P}$ is undoubtedly the ultraviolet cutoff scale of the theory thanks to the absence of large coefficients in the K's. Recall that such large coefficients are used in models of induced-gravity [10,31,32,35–37] or non-minimal [48,49] inflation and the aforementioned scale has to be determined after an expansion of $\mathcal{A}$ in Equation (4a) about $\langle\phi\rangle$.

In order to delineate the available parameter space of HSI for the two selected n values we plot its predictions in the $n_{\rm s} - r$ plane against the observational data see (Figure 4). To accomplish it, we enforce the constraints in Equation (49) varying N for several $n_{\rm d}$ values. Namely, for both n values considered, we fix $n_{\rm d} = 1$ (dashed lines), $n_{\rm d} = n$ (solid lines) or $n_{\rm d} = 2n - 1$ (dot-dashed lines). Comparing the structure of these plots with that of Figure 1 we see that this is pretty stable. The $n_{\rm s}$ values lie close to its central value in Equation (53) with a slight augmentation with $n_{\rm d}$. The r values increase with N, whose maximum increases with $n_{\rm d}$. Considering the maximum on N for any allowed $n_{\rm d}$, we show the allowed (shaded) regions in the $n_{\rm d} - N$ plane for the two considered n values in Figure 5. The findings are similar to those in Figure 2 with a decrease in the maximal N's and an increase in the maximal $n_{\rm d}$'s depicted by a dashed and a solid line, respectively. Obviously, the maximal of the maximal N values are obtained at the intersection of the dashed and the vertical solid lines.

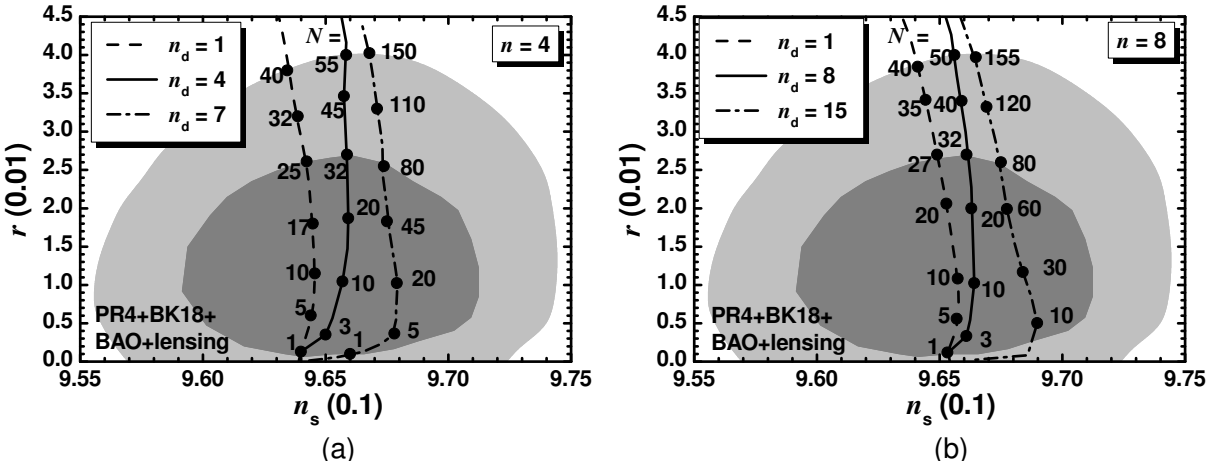

Figure 4. Curves allowed by Equation (49) in the $n_{\rm s} - r$ plane for HSI with $\langle M_X\rangle = M_{\rm GUT}$ and various N's indicated along them. We take (**a**) $n = 4$ and $n_{\rm d} = 1$ (dashed line), $n_{\rm d} = 4$ (solid line), or $n_{\rm d} = 7$ (dot-dashed line) or (**b**) $n = 8$, $n_{\rm d} = 1$ (dashed line), $n_{\rm d} = 8$ (solid line), or $n_{\rm d} = 15$ (dot-dashed line). The shaded regions are identified as in Figure 1.

Summarizing our results for $n = 4$ (see Figure 5a) we arrive at the following allowed ranges:

$$1 \lesssim N \lesssim 165, \quad 0 \leq n_{\rm d} \leq 7.99, \quad 0.964 \lesssim n_{\rm s} \lesssim 0.968 \quad \text{and} \quad 1 \lesssim \Delta_\star/100 \lesssim 41 \tag{55a}$$

with $w_{\rm rh} \simeq 0.3$, $\alpha_{\rm s} \simeq -(5.8 - 6.5)\cdot 10^{-4}$ and $N_\star \simeq (54 - 56)$. Moreover, M and $\widehat{m}_{\rm I}$ range as follows

$$3.6\ \text{YeV} \lesssim M \lesssim 43\ \text{YeV} \quad \text{and} \quad 47\ \text{EeV} \lesssim \widehat{m}_{\rm I} \lesssim 1.8\ \text{ZeV}. \tag{55b}$$

On the other hand, for $n = 8$ (see Figure 5b) we obtain

$$1 \lesssim N \lesssim 152, \quad 0 \leq n_{\rm d} \leq 15.99, \quad 0.964 \lesssim n_{\rm s} \lesssim 0.969 \quad \text{and} \quad 1 \lesssim \Delta_\star/100 \lesssim 30 \tag{56a}$$

with $w_{\rm rh} \simeq 0.5$, $\alpha_{\rm s} \simeq -(5.3-6.2)\cdot 10^{-4}$ and $N_\star \simeq (57-59)$. With regard to the mass parameters,

$$4.8\ \text{ZeV} \lesssim M \lesssim 0.17\ \text{YeV} \quad \text{and} \quad 0.16\ \text{PeV} \lesssim \widehat{m}_{\rm I} \lesssim 3.4\ \text{EeV}. \tag{56b}$$

In both Equations (55b) and (56b), the maximal values are obtained for the lowest N and the largest $n_{\rm d}$ values, whereas the minimal values are achieved at the largest N and the lowest $n_{\rm d}$ values.

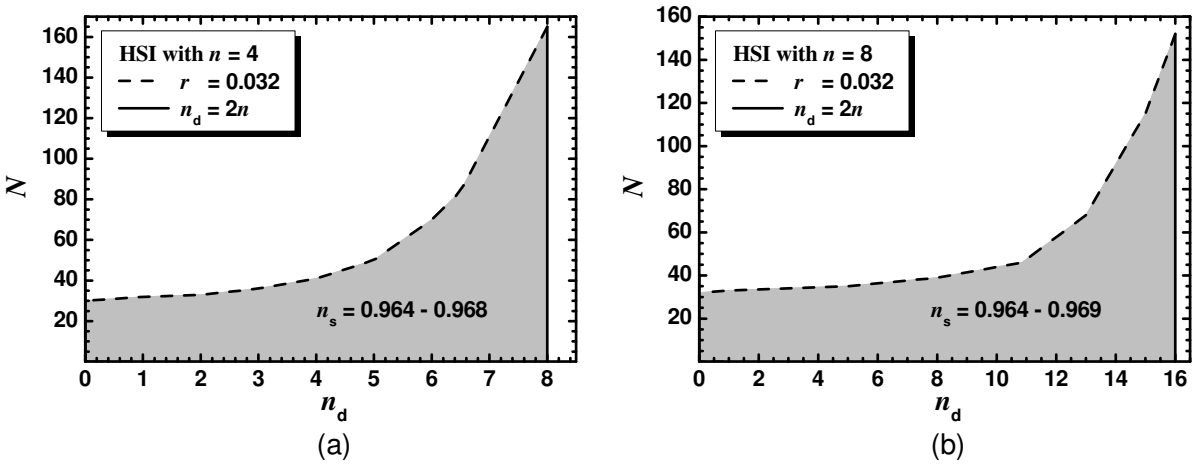

Figure 5. Allowed (shaded) region as determined by Equations (49) and (53) in the $n_{\rm d} - N$ plane for HSI with $\langle M_{\rm X}\rangle = M_{\rm GUT}$ and (**a**) $n = 4$ or (**b**) $n = 8$. The conventions adopted for the boundary lines are also shown.

6. Conclusions

We presented a novel implementation of SI (i.e., Starobinsky inflation) in the context of SUGRA, confining ourselves to models displaying a scalar potential shown in Equation (3) and a kinetic mixing in the inflaton sector with a pole of order two (see Equation (2)). We considered two classes of models—CSI, i.e., chaotic SI and HSI, i.e., Higgs SI—depending on whether the inflaton is included into a gauge-singlet or two gauge-non-singlet fields. CSI and HSI rely on the superpotentials in Equations (14) and (24), respectively, which respect an R symmetry and include an inflaton-accompanying field which facilitates the establishment of SI. On the other hand, the Kähler potential's respect the R and gauge symmetries and parameterize hyperbolic internal geometries met in T-model inflationary settings. Namely, K for CSI is given in Equation (16) whereas for HSI we considered the two distinct K's shown in Equation (28). The Higgsflaton in the last case implements the breaking of a gauge $U(1)_X$ symmetry at a scale which may assume a value compatible with the MSSM unification. All the models excellently match with the observations by restricting the free parameters to reasonably ample regions of values. In particular, $n_{\rm s}$ lies close to its central observational value while r increases with N (see Equation (54a) for CSI and Equations (55a) and (56a) for HSI). The present data on δ_{21} and the self-consistency of the models allow us to delineate the overall allowed regions for selected values of the exponent n in Equation (3) (see Figures 2 and 5). The resulting allowed margin of $n_{\rm s}$ is extended from 0.961 up to 0.969, depending on the chosen n, and therefore it is less restrictive than the corresponding prediction of the traditional Starobinsky model in Equation (48), i.e., $n_{\rm s} \simeq 0.963$. Hopefully, a more accurate determination of $n_{\rm s}$ and r in future experiments [94–97] will assist us in singling out the most favorable one from the proposed models.

The central message of our work is that SI is not exclusively implemented by the E-model kinetic mixing in Equation (1). It is also attainable via T-model normalization in Equation (2) if it is considered in conjunction with the potential in Equation (3). The method applied for the construction of our models can be extended to other SUGRA models as those motivated by D branes [98] or those which assist to obtain de Sitter vacua in line with current LHC results on SUSY as in refs. [57,65]. Moreover, it can be employed for supersymmetrizing models obtained adopting the Palatini approach to gravity [99–101].

We expect that our models of HSI admit a post-inflationary completion along the lines of refs. [31,36,37,48,68] since the mass parameters in those models are similar to those found in Equations (55b) and (56b). Regarding the ultraviolet completion, it would be interesting to investigate if our models belong to the string landscape or swampland [102]. Note that the swampland string conjectures are generically not satisfied in SUGRA-based models [103,104], but there are suggestions [105–107] which may use in our framework as well.

Funding: This research received no external funding.

Data Availability Statement: Data are contained within the article.

Acknowledgments: I would like to thank I. Ben-Dayan, S. Ketov, and V. Zarikas for useful discussions related to the Killing-adapted coordinates.

Conflicts of Interest: The author declares no conflicts of interest.

Appendix A. Shift Symmetry & Hyperbolic Kähler Geometries

We here demonstrate that the inflaton-sector Kähler potentials employed for $n_{\rm d} = 0$ in our work exhibits a shift symmetry together with its original hyperbolic structure; this has already been extensively discussed in refs. [56,57,66]. To accomplish our goal, we first find the matrix form of the Kähler metric

$$\mathbf{M}_K = \left(K_{\alpha\bar{\beta}}\right) \text{ with } z^\alpha = \begin{cases} \Phi & \text{for } K = \widetilde{K}_{11}, \\ \bar{\Phi}, \Phi & \text{for } K = \widetilde{K}_{(11)^2} \text{ and } \widetilde{K}_{21}. \end{cases} \tag{A1}$$

We then introduce the so-called Killing-adapted coordinates [56,57] and express our K's in terms of them attempting to reveal a shift symmetry along the inflationary paths of Equation (13) or (23). We concentrate first on SI with a gauge-singlet inflaton (see Appendix A.1) and then with a gauge-non-singlet inflaton (see Appendix A.2).

Appendix A.1. Shift Symmetry for CSI

We concentrate on the following part of $\widetilde{K}_{2(11)^2{\rm d}}$ in Equation (16)

$$\widetilde{K}_{11} = -N \ln \frac{(1-|\Phi|^2)}{(1-\Phi^2)^{1/2}(1-\Phi^{*2})^{1/2}}, \tag{A2}$$

which parameterizes $SU(1,1)/U(1)$ with curvature ${\rm R}_{11} = -2/N$. The Kähler metric is a trivial 1×1 matrix with element

$$\mathbf{M}_{11} = N/(1-|\Phi|^2)^2. \tag{A3}$$

We then introduce the superfield Ψ via the relation

$$\Phi = \tanh \frac{\Psi}{\sqrt{2N}}. \tag{A4}$$

Note that Ψ coincides with canonically normalized inflaton in Equation (19). Inserting it into Equation (A2), $\widetilde{K}_{11}$ can be brought into the form

$$\widetilde{K}_{11} = -N \ln \cosh \frac{\Psi - \Psi^*}{\sqrt{2N}}, \tag{A5}$$

if we take into account the identities of the hyperbolic functions

$$\cosh(x-y) = \cosh x \cosh y (1 - \tanh x \tanh y) \;\text{ and }\; \cosh x = (1 - \tanh x)^{-1/2}. \tag{A6}$$

From the expression in Equation (A5), it is clear that $\widetilde{K}_{11}$ is invariant under the shift symmetry

$$\Psi \to \Psi + c \;\text{ with }\; c \in \mathbb{R}. \tag{A7}$$

Therefore, $\widetilde{K}_{11}$ is independent of the canonically normalized inflaton $\widehat{\phi}$ in Equation (2) which can be identified as the real part of Ψ.

Appendix A.2. Shift Symmetry for HSI

We specify the emergence of a shift symmetry in the two K's used for HSI in Equation (26).

Appendix A.2.1. Kähler Manifold $\mathcal{M}_{(11)^2}$

We concentrate on the inflationary contribution to $\widetilde{K}_{2(11)^2\mathrm{d}}$ in Equation (26) which reads

$$\widetilde{K}_{(11)^2} = -\frac{N}{2} \ln \frac{(1 - 2|\Phi|^2)(1 - 2|\bar{\Phi}|^2)}{(1 - 2\bar{\Phi}\Phi)(1 - 2\bar{\Phi}^*\Phi^*)} \tag{A8}$$

and parameterizes $\mathcal{M}_{(11)^2} = (SU(1,1)/U(1))^2$ with curvature $\mathsf{R}_{(11)^2} = -4/(N/2)$. The Kähler metric can be represented as a diagonal 2×2 matrix

$$\mathbf{M}_{(11)^2} = N \mathsf{diag}\Big((1 - |\Phi|^2)^{-2}, (1 - |\bar{\Phi}|^2)^{-2}\Big). \tag{A9}$$

working along the lines of the previous section, we introduce two superfields Ψ and $\bar{\Psi}$ via the relations

$$\Phi = \frac{1}{\sqrt{2}} \tanh \frac{\Psi}{\sqrt{2N}} \;\text{ and }\; \bar{\Phi} = \frac{1}{\sqrt{2}} \tanh \frac{\bar{\Psi}}{\sqrt{2N}}. \tag{A10}$$

Upon substitution into Equation (A8), $\widetilde{K}_{(11)^2}$ can be brought into the form

$$\widetilde{K}_{(11)^2} = -\frac{N}{2} \ln \frac{\cosh \frac{\Psi - \Psi^*}{\sqrt{2N}} \cosh \frac{\bar{\Psi} - \bar{\Psi}^*}{\sqrt{2N}}}{\cosh \frac{\Psi - \bar{\Psi}}{\sqrt{2N}} \cosh \frac{\bar{\Psi}^* - \Psi^*}{\sqrt{2N}}}. \tag{A11}$$

Taking into account that along the inflationary trough in Equation (23) $\Phi = \bar{\Phi}$ and so $\Psi = \bar{\Psi}$, the expression above reduces to the following:

$$\widetilde{K}_{(11)^2}\Big|_{\text{Equation (23)}} = -\frac{N}{2} \ln \cosh^2 \frac{\Psi - \Psi^*}{\sqrt{2N}}. \tag{A12}$$

Consequently, $K_{(11)^2}$ is invariant under the shift symmetry of Equation (A7) and independent of $\mathsf{Re}\Psi = \mathsf{Re}\bar{\Psi}$ i.e., $\widehat{\phi}$ (see Equations (2) and (32a)).

Appendix A.2.2. Kähler Manifold $\mathcal{M}_{21}$

Here, we focus on the inflationary contribution to $\widetilde{K}_{221\mathrm{d}}$ in Equation (26), which reads

$$\widetilde{K}_{21} = -N \ln \frac{1-|\Phi|^2-|\bar{\Phi}|^2}{(1-2\bar{\Phi}\Phi)^{1/2}(1-2\bar{\Phi}^*\Phi^*)^{1/2}}, \tag{A13}$$

which parameterizes $\mathcal{M}_{21} = SU(2,1)/U(1)$ with a curvature $\mathsf{R}_{21} = -6/N$. The Kähler metric is a non-diagonal 2×2 matrix

$$\mathbf{M}_{21} = \frac{N}{F_{\mathrm{T}}^2}\begin{pmatrix} 1-|\bar{\Phi}|^2 & \Phi^*\bar{\Phi} \\ \Phi\bar{\Phi}^* & 1-|\Phi|^2 \end{pmatrix}, \tag{A14}$$

where F_{T} is given in Equation (25). The introduction of the Killing-adapted coordinates can be now performed after diagonalizing $\mathbf{M}_{21}$. This can be performed via a similarity transformation involving a hermitian matrix U_{21} as follows:

$$U_{21}^\dagger \mathbf{M}_{21} U_{21} = \mathsf{diag}(\kappa_+,\kappa_-) \;\text{ with }\; U_{21} = \frac{1}{\sqrt{|\Phi|^2+|\bar{\Phi}|^2}}\begin{pmatrix} |\bar{\Phi}|\Phi^*/\bar{\Phi}^* & -|\Phi|\bar{\Phi}/\Phi \\ |\bar{\Phi}| & |\Phi| \end{pmatrix}. \tag{A15}$$

The eigenvectors and eigenvalues of $\mathbf{M}_{21}$ are given, respectively, by

$$\begin{pmatrix} \dot{\Phi}_+ \\ \dot{\Phi}_- \end{pmatrix} = U_{21}^\dagger \begin{pmatrix} \dot{\Phi} \\ \dot{\bar{\Phi}} \end{pmatrix} \quad \text{and} \quad \begin{cases} \kappa_+ = N/F_{\mathrm{T}}^2, \\ \kappa_- = N/F_{\mathrm{T}}. \end{cases} \tag{A16}$$

It is very difficult, if not impossible, to integrate the relations above so as to determine generically Φ and $\bar{\Phi}$ in terms of $\Phi_\pm$. Therefore, we are not able to obtain a generic formula for $\widetilde{K}_{21}$ as in Equation (A11) for $\widetilde{K}_{(11)^2}$. However, confining ourselves along the direction in Equation (23) and integrating the relevant relations in Equation (A16) with respect to the cosmic time, we find

$$\Phi_+ = (\bar{\Phi}+\Phi)/\sqrt{2} \quad \text{and} \quad \Phi_- = (\bar{\Phi}-\Phi)/\sqrt{2}. \tag{A17}$$

Solving the system above with respect to $(\bar{\Phi},\Phi)$ and taking into account that $\langle\Phi_-\rangle_{\mathrm{I}} = 0$ (see Equations (22) and (23)), we obtain

$$\widetilde{K}_{21}\Big|_{\text{Equation (23)}} = -N \ln \frac{1-|\Phi_+|^2}{(1-\Phi_+^2)^{1/2}(1-\Phi_+^2)^{1/2}}. \tag{A18}$$

We introduce again a new holomorphic variable Ψ_+ via the relation

$$\Phi_+ = \tanh\frac{\Psi_+}{\sqrt{2N}}. \tag{A19}$$

During HSI, Ψ_+ becomes the real canonical variable $\widehat{\phi}$ (see Equations (2) and (32a)). Inserting it in Equation (A18), it can be brought into the form

$$\widetilde{K}_{21}\Big|_{\text{Equation (23)}} = -N \ln\cosh\frac{\Psi_+-\Psi_+^*}{\sqrt{2N}}. \tag{A20}$$

This result manifests the invariance of $\widetilde{K}_{21}$ under the transformation of Equation (A7) with Ψ replaced by Ψ_+ and so $\widetilde{K}_{21}$ is independent from $\mathsf{Re}\Psi_+ = \widehat{\phi}$ (see Equations (22) and (A17)).

References

1. Starobinsky, A.A. A New Type of Isotropic Cosmological Models Without Singularity. *Phys. Lett. B* **1980**, *91*, 99–102. [CrossRef]
2. Martin, J.; Ringeval, C.; Vennin, V. Encyclopædia Inflationaris. *Phys. Dark Univ.* **2014**, *5*, 75. [CrossRef]
3. Martin, J.; Ringeval, C.; Trotta, R.; Vennin, V. The Best Inflationary Models After Planck. *J. Cosmol. Astropart. Phys.* **2014**, *03*, 39. [CrossRef]
4. Grøn, Ø. Predictions of Spectral Parameters by Several Inflationary Universe Models in Light of the Planck Results. *Universe* **2018**, *4*, 15. [CrossRef]
5. Akrami, Y. et al. [Planck Collaboration]. Planck 2018 results. X. Constraints on inflation. *Astron. Astrophys.* **2020**, *641*, A10.
6. Kounnas, C.; Lüst, D.; Toumbas, N. R^2 inflation from scale invariant supergravity and anomaly free superstrings with fluxes. *Fortsch. Phys.* **2015**, *63*, 12. [CrossRef]
7. Galante, M.; Kallosh, R.; Linde, A.; Roest, D. Unity of Cosmological Inflation Attractors. *Phys. Rev. Lett.* **2015**, *114*, 141302. [CrossRef]
8. Ellis, J.; Nanopoulos, D.V.; Olive, K.A.; Verner, S. A general classification of Starobinsky-like inflationary avatars of $SU(2,1)/SU(2) \times U(1)$ no-scale supergravity. *J. High Energy Phys.* **2019**, *3*, 099. [CrossRef]
9. Ellis, J.; Garcia, M.A.G.; Nagata, N.; Nanopoulos, D.V.; Olive, K.A.; Verner, S. Building Models of Inflation in No-Scale Supergravity. *Int. J. Mod. Phys. D* **2020**, *16*, 2030011. [CrossRef]
10. Pallis, C.; Toumbas, N. Starobinsky Inflation: From Non-SUSY To SUGRA Realizations. *Adv. High Energy Phys.* **2017**, *2017*, 6759267. [CrossRef]
11. Binétruy, P. *Supersymmetry: Theory, Experiment and Cosmology*; Oxford University Press: Oxford, UK, 2006.
12. Navas, S. et al. [Particle Data Group]. Review of particle physics. *Phys. Rev. D* **2024**, *110*, 030001. [CrossRef]
13. Wang, F.; Wang, W.; Yang, J.; Zhang, Y.; Zhu, B. Low Energy Supersymmetry Confronted with Current Experiments: An Overview. *Universe* **2022**, *8*, 178. [CrossRef]
14. Buchmüller, W.; Domcke, V.; Kamada, K. The Starobinsky Model from Superconformal D-Term Inflation. *Phys. Lett. B* **2013**, *726*, 467. [CrossRef]
15. Basilakos, S.; Mavromatos, N.E.; Sola, J. Starobinsky-like inflation and running vacuum in the context of Supergravity. *Universe* **2016**, *2*, 14. [CrossRef]
16. Ketov, S.V.; Starobinsky, A.A. Embedding $(R + R^2)$-Inflation into Supergravity. *Phys. Rev. D* **2011**, *83*, 063512. [CrossRef]
17. Blumenhagen, R.; Font, A.; Fuchs, M.; Herschmann, D.; Plauschinn, E. Towards axionic Starobinsky-like inflation in string theory. *Phys. Lett. B* **2015**, *746*, 217. [CrossRef]
18. Li, T.; Li, Z.; Nanopoulos, D.V. Helical phase inflation via non-geometric flux compactifications: From natural to Starobinsky-like inflation. *J. High Energy Phys.* **2015**, *10*, 138. [CrossRef]
19. Ellis, J.; Nanopoulos, D.V.; Olive, K.A. No-Scale Supergravity Realization of the Starobinsky Model of Inflation. *Phys. Rev. Lett.* **2013**, *111*, 111301; Erratum in *Phys. Rev. Lett.* **2013**, *111*, 129902. [CrossRef]
20. Ellis, J.; Nanopoulos, D.V.; Olive, K. Starobinsky-like Inflationary Models as Avatars of No-Scale Supergravity. *J. Cosmol. Astropart. Phys.* **2013**, *10*, 009. [CrossRef]
21. Ellis, J.; He, H.-J.; Xianyu, Z.-Z. New Higgs inflation in a no-scale supersymmetric SU(5) GUT. *Phys. Rev. D* **2015**, *91*, 021302. [CrossRef]
22. Garg, I.; Mohanty, S. No-scale SUGRA SO(10) derived Starobinsky model of inflation. *Phys. Lett. B* **2015**, *751*, 7. [CrossRef]
23. Ellis, J.; Garcia, M.A.G.; Nagata, N.; Nanopoulos, D.V.; Olive, K.A. Starobinsky-like Inflation, Supercosmology and Neutrino Masses in No-Scale Flipped SU(5). *J. Cosmol. Astropart. Phys.* **2017**, *7*, 006. [CrossRef]
24. Ellis, J.; Garcia, M.A.G.; Nagata, N.; Nanopoulos, D.V.; Olive, K.A. Starobinsky-Like Inflation and Neutrino Masses in a No-Scale SO(10) Model. *J. Cosmol. Astropart. Phys.* **2016**, *11*, 018. [CrossRef]
25. Cremmer, E.; Ferrara, S.; Kounnas, C.; Nanopoulos, D.V. Naturally Vanishing Cosmological Constant in $N = 1$ Supergravity. *Phys. Lett. B* **1983**, *133*, 61. [CrossRef]
26. Lahanas, A.B.; Nanopoulos, D.V. The Road to No-Scale Supergravity. *Phys. Rept.* **1987**, *145*, 198. [CrossRef]
27. Cecotti, S. Higher Derivative Supergravity Is Equivalent To Standard Supergravity Coupled To Matter. *Phys. Lett. B* **1987**, *190*, 86. [CrossRef]
28. Farakos, F.; Kehagias, A.; Riotto, A. On the Starobinsky Model of Inflation from Supergravity. *Nucl. Phys.* **2013**, *B876*, 187. [CrossRef]
29. Kallosh, R.; Linde, A. Superconformal generalizations of the Starobinsky model. *J. Cosmol. Astropart. Phys.* **2013**, *6*, 28. [CrossRef]
30. Lahanas, A.B.; Tamvakis, K. Inflation in no-scale supergravity. *Phys. Rev. D* **2015**, *91*, 085001. [CrossRef]
31. Pallis, C. Linking Starobinsky-Type Inflation in no-Scale Supergravity to MSSM. *J. Cosmol. Astropart. Phys.* **2014**, *4*, 024; Erratum in *J. Cosmol. Astropart. Phys.* **2017**, *7*, 01(E). [CrossRef]
32. Pallis, C. Induced-Gravity Inflation in no-Scale Supergravity and Beyond. *J. Cosmol. Astropart. Phys.* **2014**, *08*, 057. [CrossRef]

33. Pallis, C. Reconciling induced-gravity inflation in supergravity with the Planck 2013 & BICEP2 results. *J. Cosmol. Astropart. Phys.* **2014**, *10*, 58.
34. Kallosh, R. More on Universal Superconformal Attractors. *Phys. Rev. D* **2014**, *89*, 087703. [CrossRef]
35. Pallis, C.; Toumbas, N. Starobinsky-Type Inflation with Products of Kähler Manifolds. *J. Cosmol. Astropart. Phys.* **2016**, *5*, 15. [CrossRef]
36. Pallis, C.; Shafi, Q. Induced-Gravity GUT-Scale Higgs Inflation in Supergravity. *Eur. Phys. J. C* **2018**, *78*, 523. [CrossRef]
37. Pallis, C. Starobinsky-Type $B-L$ Higgs Inflation Leading Beyond MSSM. *arXiv* **2023**, arXiv:2305.00523.
38. Kallosh, R.; Linde, A.; Rube, T. General inflaton potentials in supergravity. *Phys. Rev. D* **2011**, *83*, 043507. [CrossRef]
39. Lee, H.M. Chaotic inflation in Jordan frame supergravity. *J. Cosmol. Astropart. Phys.* **2010**, *08*, 003. [CrossRef]
40. Antoniadis, I.; Dudas, E.; Ferrara, S.; Sagnotti, A. The Volkov—Akulov—Starobinsky Supergravity. *Phys. Lett. B* **2014**, *733*, 32. [CrossRef]
41. Aldabergenov, Y. Volkov–Akulov–Starobinsky supergravity revisited. *Eur. Phys. J. C* **2020**, *80*, 329. [CrossRef]
42. Ferrara, S.; Kallosh, R.; Linde, A. Cosmology with Nilpotent Superfields. *J. High Energy Phys.* **2014**, *10*, 143. [CrossRef]
43. Antoniadis, I.; Nanopoulos, D.V.; Olive, K.A. R^2–Inflation Derived from 4d Strings, the Role of the Dilaton, and Turning the Swampland into a Mirage. *arXiv* **2024**, arXiv:2410.16541.
44. Zee, A. A Broken Symmetric Theory of Gravity. *Phys. Rev. Lett.* **1979**, *42*, 417. [CrossRef]
45. Giudice, G.F.; Lee, H.M. Starobinsky-like inflation from induced gravity. *Phys. Lett. B* **2014**, *733*, 58. [CrossRef]
46. Pallis, C.; Shafi, Q. Non-minimal chaotic inflation, Peccei-Quinn phase transition and non-thermal leptogenesis. *Phys. Rev. D* **2012**, *86*, 023523. [CrossRef]
47. Pallis, C.; Shafi, Q. Gravity Waves From Non-Minimal Quadratic Inflation. *J. Cosmol. Astropart. Phys.* **2015**, *3*, 23. [CrossRef]
48. Pallis, C. Unitarity-Safe Models of Non-Minimal Inflation in Supergravity. *Eur. Phys. J. C* **2018**, *78*, 1014. [CrossRef]
49. Pallis, C. Unitarizing non-Minimal Inflation via a Linear Contribution to the Frame Function. *Phys. Lett. B* **2019**, *789*, 243. [CrossRef]
50. Kehagias, A.; Dizgah, A.M.; Riotto, A. Remarks on the Starobinsky model of in ation and its descendants. *Phys. Rev. D* **2014**, *89*, 043527. [CrossRef]
51. Terada, T. Generalized Pole Inflation: Hilltop, Natural, and Chaotic Inflationary Attractors. *Phys. Lett. B* **2016**, *760*, 674. [CrossRef]
52. Broy, B.J.; Galante, M.; Roest, D.; Westphal, A. Pole inflation, Shift symmetry and universal corrections. *J. High Energy Phys.* **2015**, *12*, 149. [CrossRef]
53. Kobayashi, T.; Seto, O.; Tatsuishi, T.H. Toward pole inflation and attractors in supergravity: Chiral matter field inflation. *Prog. Theor. Phys.* **2017**, *2017*, 123B04. [CrossRef]
54. Pallis, C. Pole Inflation in Supergravity. *PoS CORFU* **2022**, *2021*, 78.
55. Karamitsos, S.; Strumia, A. Pole inflation from non-minimal coupling to gravity. *J. High Energy Phys.* **2022**, *2022*, 16. [CrossRef]
56. Carrasco, J.J.M.; Kallosh, R.; Linde, A.; Roest, D. Hyperbolic geometry of cosmological attractors. *Phys. Rev. D* **2015**, *92*, 041301. [CrossRef]
57. Carrasco, J.J.M.; Kallosh, R.; Linde, A. α-Attractors: Planck, LHC and Dark Energy. *J. High Energy Phys.* **2015**, *10*, 147. [CrossRef]
58. Pallis, C. An Alternative Framework for E-Model Inflation in Supergravity. *Eur. Phys. J. C* **2022**, *82*, 444. [CrossRef]
59. Kallosh, R.; Linde, A.; Roest, D. Superconformal Inflationary α-Attractors. *J. High Energy Phys.* **2013**, *11*, 198. [CrossRef]
60. Kallosh, R.; Linde, A. Universality Class in Conformal Inflation. *J. Cosmol. Astropart. Phys.* **2013**, *2013*, 002. [CrossRef]
61. Kallosh, R.; Linde, A. BICEP/Keck and cosmological attractors. *J. Cosmol. Astropart. Phys.* **2021**, *2021*, 1–13. [CrossRef]
62. Ellis, J.; Garcia, M.A.G.; Nanopoulos, D.V.; Olive, K.A.; Verner, S. BICEP/Keck constraints on attractor models of inflation and reheating. *Phys. Rev. D* **2022**, *105*, 043504. [CrossRef]
63. Bhattacharya, S.; Dutta, K.; Gangopadhyay, M.R.; Maharana, A. α-attractor inflation: Models and predictions. *Phys. Rev. D* **2023**, *107*, 103530. [CrossRef]
64. Dimopoulos, K. *Introduction to Cosmic Inflation and Dark Energy*; CRC Press: Boca Raton, FL, USA, 2020; ISBN 978-0-367-61104-0.
65. Ellis, J.; Nanopoulos, D.V.; Olive, K.A.; Verner, S. Unified No-Scale Attractors. *J. Cosmol. Astropart. Phys.* **2019**, *9*, 40. [CrossRef]
66. Pallis, C. Pole-induced Higgs inflation with hyperbolic Kähler geometries. *J. Cosmol. Astropart. Phys.* **2021**, *5*, 43. [CrossRef]
67. Pallis, C. $SU(2,1)/(SU(2)\times U(1))$ B-L Higgs Inflation. *J. Phys. Conf. Ser.* **2021**, *2105*, 12. [CrossRef]
68. Pallis, C. T-Model Higgs Inflation in Supergravity. *arXiv* **2023**, arXiv:2307.14652.
69. Hooft, G. Naturalness, chiral symmetry, and spontaneous chiral symmetry breaking. *NATO Sci. Ser. B* **1980**, *59*, 135.
70. Kawasaki, M.; Yamaguchi, M.; Yanagida, T. Natural chaotic inflation in supergravity. *Phys. Rev. Lett.* **2000**, *85*, 3572. [CrossRef]
71. Brax, P.; Martin, J. Shift symmetry and inflation in supergravity. *Phys. Rev. D* **2005**, *72*, 023518. [CrossRef]
72. Antusch, S.; Dutta, K.; Kostka, P.M. SUGRA Hybrid Inflation with Shift Symmetry. *Phys. Lett. B* **2009**, *677*, 221. [CrossRef]
73. Li, T.; Li, Z.; Nanopoulos, D.V. Supergravity Inflation with Broken Shift Symmetry and Large Tensor-to-Scalar Ratio. *J. Cosmol. Astropart. Phys.* **2014**, *2*, 028. [CrossRef]
74. Pallis, C. Kinetically modified nonminimal chaotic inflation. *Phys. Rev. D* **2015**, *91*, 123508. [CrossRef]

75. Pallis, C. Kinetically Modified Non-Minimal Inflation with Exponential Frame Function. *Eur. Phys. J. C* **2017**, 77, 633. [CrossRef]
76. Ben-Dayan, I.; Einhorn, M.B. Supergravity Higgs Inflation and Shift Symmetry in Electroweak Theory. *J. Cosmol. Astropart. Phys.* **2010**, *12*, 002. [CrossRef]
77. Lazarides, G.; Pallis, C. Shift Symmetry and Higgs Inflation in Supergravity with Observable Gravitational Waves. *J. High Energy Phys.* **2015**, *11*, 114. [CrossRef]
78. Pallis, C. Kinetically modified nonminimal Higgs inflation in supergravity. *Phys. Rev. D* **2015**, *92*, 121305. [CrossRef]
79. Pallis, C. Variants of Kinetically Modified Non-Minimal Higgs Inflation in Supergravity. *J. Cosmol. Astropart. Phys.* **2016**, *10*, 37. [CrossRef]
80. Kallosh, R.; Linde, A.; Roest, D.; Wrase, T. Sneutrino inflation with α-attractors. *J. Cosmol. Astropart. Phys.* **2016**, *11*, 046. [CrossRef]
81. Gonzalo, T.E.; Heurtier, L.; Moursy, A. Sneutrino driven GUT Inflation in Supergravity. *J. High Energy Phys.* **2017**, *6*, 109. [CrossRef]
82. Kaneta, K.; Mambrini, Y.; Olive, K.A.; Verner, S. Inflation and Leptogenesis in High-Scale Supersymmetry. *Phys. Rev. D* **2020**, *101*, 015002. [CrossRef]
83. Ellis, J.; Garcia, M.A.G.; Nanopoulos, D.V.; Olive, K.A. Phenomenological aspects of no-scale inflation models. *J. Cosmol. Astropart. Phys.* **2015**, *10*, 3. [CrossRef]
84. Ema, Y.; Garcia, M.A.G.; Ke, W.; Olive, K.A.; Verner, S. Inflaton Decay in No-Scale Supergravity and Starobinsky-like Models. *Universe* **2024**, *10*, 239. [CrossRef]
85. Pallis, C. T-Model Higgs Inflation and Metastable Cosmic Strings. *J. High Energy Phys.* **2025**, *1*, 178. [CrossRef]
86. Pallis, C. E- and T-model hybrid inflation. *Eur. Phys. J. C* **2023**, *83*, 2. [CrossRef]
87. Aghanim, N. et al. [Planck Collaboration]. Planck 2018 results. VI. Cosmological parameters. *Astron. Astrophys.* **2020**, *641*, A6; Erratum in *Astron. Astrophys.* **2021**, *652*, C4.
88. Martin, J.; Ringeval, C. First CMB Constraints on the Inflationary Reheating Temperature. *Phys. Rev. D* **2010**, *82*, 023511. [CrossRef]
89. Ellis, J.; Garcia, M.A.G.; Nanopoulos, D.V.; Olive, K.A. Calculations of Inflaton Decays and Reheating: With Applications to No-Scale Inflation Models. *J. Cosmol. Astropart. Phys.* **2015**, *7*, 50. [CrossRef]
90. Lin, C.M. On the oscillations of the inflaton field of the simplest α-attractor T-model. *Chin. J. Phys.* **2023**, *86*, 323. [CrossRef]
91. Turner, M.S. Coherent Scalar-Field Oscillations in an Expanding Universe. *Phys. Rev. D* **1983**, *28*, 1243. [CrossRef]
92. Tristram, M.; Banday, M.J.; Górski, K.M.; Keskitalo, R.; Lawrence, C.R.; Andersen, K.J.; Barreiro, R.B.; Borrill, J.; Colombo, L.P.L.; Eriksen, H.K.; et al. Improved limits on the tensor-to-scalar ratio using BICEP and Planck. *Phys. Rev. Lett.* **2021**, *127*, 151301. [CrossRef]
93. Ade, P.A.R. et al. [BICEP and Keck Collaboration]. Improved Constraints on Primordial Gravitational Waves using Planck, WMAP, and BICEP/Keck Observations through the 2018 Observing Season. *Phys. Rev. Lett.* **2021**, *127*, 151301. [CrossRef] [PubMed]
94. Abazajian, K.; Addison, G.E.; Adshead, P.; Ahmed, Z.; Allen, S.W.; Alonso, D.; Alvarez, M.; Anderson, A.; Arnold, K.S.; Baccigalupi, C.; et al. CMB-S4 Science Case, Reference Design, and Project Plan. *arXiv* **2019**, arXiv:1907.04473.
95. Andre, P. et al. [PRISM Collaboration]. PRISM (Polarized Radiation Imaging and Spectroscopy Mission): A White Paper on the Ultimate Polarimetric Spectro-Imaging of the Microwave and Far-Infrared Sky. *arXiv* **2013**, arXiv:1306.2259.
96. Montier, L. et al. [LiteBIRD Collaboration]. Overview of the Medium and High Frequency Telescopes of the LiteBIRD satellite mission. *Proc. SPIE Int. Soc. Opt. Eng.* **2020**, *11443*, 114432G.
97. Baumann, D. et al. [CMBPol Study Team Collaboration]. CMBPol Mission Concept Study: Probing Inflation with CMB Polarization. *AIP Conf. Proc.* **2009**, *1141*, 10.
98. Kallosh, R.; Linde, A. Polynomial α-attractors. *J. Cosmol. Astropart. Phys.* **2022**, *4*, 17. [CrossRef]
99. Bauer, F.; Demir, D.A. Higgs-Palatini Inflation and Unitarity. *Phys. Lett. B* **2011**, *698*, 425. [CrossRef]
100. Enckell, V.M.; Enqvist, K.; Rasanen, S.; Wahlman, L.P. Inflation with R^2 term in the Palatini formalism. *J. Cosmol. Astropart. Phys.* **2019**, *2*, 22. [CrossRef]
101. Antoniadis, I.; Karam, A.; Lykkas, A.; Tamvakis, K. Palatini inflation in models with an R^2 term. *J. Cosmol. Astropart. Phys.* **2018**, *11*, 28. [CrossRef]
102. Vafa, C. The String landscape and the swampland. *arXiv* **2005**, arXiv:hep-th/0509212.
103. Garg, S.K.; Krishnan, C. Bounds on Slow Roll and the de Sitter Swampland. *J. High Energy Phys.* **2019**, *11*, 75. [CrossRef]
104. Ooguri, H.; Palti, E.; Shiu, G.; Vafa, C. Distance and de Sitter Conjectures on the Swampland. *Phys. Lett. B* **2019**, *788*, 180. [CrossRef]
105. Ferrara, S.; Tournoy, M.; Van Proeyen, A. de Sitter Conjectures in N=1 Supergravity. *Fortsch. Phys.* **2020**, *68*, 1900107. [CrossRef]
106. Atli, U.; Guleryuz, O. A Solution to the de Sitter Swampland Conjecture versus Inflation Tension via Supergravity. *J. Cosmol. Astropart. Phys.* **2021**, *4*, 27. [CrossRef]
107. Rasulian, I.M.; Torabian, M.; Velasco-Sevilla, L. Swampland de Sitter conjectures in no-scale supergravity models. *Phys. Rev. D* **2021**, *104*, 044028. [CrossRef]